ADDIS ABABA UNIVERSITY

ADDIS ABABA INSTITUTE OF TECHNOLOGY

(AAiT)

SCHOOL OF GRADUATE STUDIES

ENERGY CENTER

ANALYSIS AND PERFORMANCE SIMULATION OF SOLAR POWERED WATER PUMPING SYSTEM: A CASE STUDY IN JIGJIGA

By:

Sofiya Hussein Arshi

A thesis submitted to the School of Graduate Studies of Addis Ababa institute of Technology in partial fulfillment of the Masters of Science in Energy Technology

*Advisor: **Yilma Tadesse (PhD)***

Date: June, 2019

Addis Ababa University

Addis Ababa Institute of Technology (AAiT)

School of Graduate Studies

Center of Energy Technology

Analysis and Performance Simulation of Solar Powered Water Pumping System: A Case Study in Jigjiga

By: Sofiya Hussein

Approved by board of examiner

Dr. Solomon T/Mariam	_____	_____
Head, Energy Center	Signature	Date
Dr. Yilma Tadesse	_____	_____
Advisor	Signature	Date
Dr. Solomon T/Mariam	_____	_____
Internal examiner	Signature	Date
Dr. Abdulkadir Aman	_____	_____
External examiner	Signature	Date

Declaration

Addis Ababa University

Addis Ababa Institute of Technology

School of Graduate Studies

This is to certify that the thesis prepared by Sofiya Hussein Arshi, Titled: "ANALYSIS AND PERFORMANCE SIMULATION OF SOLAR POWERED WATER PUMPING SYSTEM: A CASE STUDY IN JIGJIGA", and submitted in partial fulfillment of the Master of Science in Energy Technology complies with the regulation of the university and meet the accepted standards with respect to originality and quality.

Signed by Examining Committee:

Dr. Solomon T/Mariam	_____	_____
Internal examiner	Signature	Date
Dr. Abdulkadir Aman	_____	_____
External examiner	Signature	Date
Dr. Yilma Tadesse	_____	_____
Advisor	Signature	Date

_____

Chair of Department of Graduate Program Coordinator

ABSTRACT

In most regions of Ethiopia groundwater is the major source of freshwater for drinking and agriculture, almost all groundwater is obtained from shallow to moderately deep wells. Whether we use diesel generators to generate power or electricity from the grid, the energy consumption is high and also using diesel energy which is one of the major causes of air pollution. The possible solution to minimize this problem is using renewable energy system. In this research the performance analysis of photovoltaic powered water pumping (PVPWP) system with maximum power point tracking (MPPT) controller was carried out under climate condition of Jigjiga. In this research a detailed electrical characteristics of 1800Watt non-tracking PV array (with 6Sx4P configuration) was determined on current vs. voltage as well as power vs. voltage plane by taking manufacturer's data sheet of the PV module as input. A polynomial performance equation (which relates output flow rate of the pump with the input power and system head) was obtained with curve fitting technique, after performance points of the pump had been taken from the performance curve. Hence the hourly performance variation of the PVPWP system was predicted from the electrical characteristics of the PV array and the performance equation for (50, 60, 70, 80, and 90 meters of pumping heads). The modeled system gives a flow rate of 20-30 m^3/day for sunny days for the total dynamic head of 80m and solar irradiation of 5000-7000 Wh/m^2/day

Keywords: Photovoltaic water Pumping system, curve fitting, MPPT controller.

ACKNOWLEDGMENT

I submit my highest appreciation to Dr. Yilma Tadesse for his timeless advice that significantly helped me in this thesis, for his continuous support, scientific discussions and for reviewing my thesis. I am deeply indebted to his continuous supervision, original ideas and guidance.

In this respect, my gratefulness is directed to my friend Elias Mesfin for his suggestion and helping attitude in my way out to timely completion of this thesis and my family for their various invaluable suggestions and support during this time.

TABLE OF CONTENTS

LIST OF FIGURE

LIST OF TABLE

NOMENCLATURE

PV	*Photovoltaic*
WPS	*Water Pumping System*
PVPWPS	*Photovoltaic powered water pumping system*
SPVPWPS	*Solar photovoltaic powered water pumping system*
EEP	*Ethiopian electric power*
MPPT	*Maximum power point tracking*
DC	*Direct current*
AC	*Alternating current*
W	*Watt*
h	*Hour*
l	*Litter*
m	*Meter*
V	*Voltage*
I	*Current*
Vmpp	*Voltage at maximum power point*
Impp	*Current at maximum power point*
I_D	*Diode current*
Ish	*Shunt current*
Rsh	*Shunt resister*
Rs	*Series resistance*
Rp	*Parallel resistance*
Voc,n	*Nominal open-circuit voltage*
Isc,n	*Nominal short-circuit current*
Vt	*Thermal voltage*
KW	*Kilowatt*
KWh	*Kilowatt hour*
MW	*Megawatt*
Q	*Flow rate*
P	*Power*
H	*Head*
TDH	*Total dynamic head*
P_H	*Hydraulic power*
P_{EL}	*Electric power*
P_{PV}	*Photovoltaic power*
g	*Gravity*
L	*Length*
D	*Diameter*
V'	*Fluid Velocity*
A	*Area*
K	*Loss coefficient*
Hg	*Global solar irradiation*
STC	*Standard test condition*

G	*Radiation intensity*
G_{GLOB}	*Global solar radiance*
G_{REF}	*Incident solar radiance*
Gn	*Nominal irradiation*
G_B	*Beam radiation*
G_D	*Diffuse radiation*
Gt	*Radiation on tilt*
G_R	*Reflected radiation*
T	*Temperature*
$NOCT$	*Nominal operating cell temperature*
Ta	*Ambient temperature*
^oC	*Degree centigrade*
N	*Any day of the year*
AST	*Apparent solar time*
LST	*Local solar time*
LSN	*Local solar noon*
SL	*Standard Longitude of the country*
LL	*Local longitude of the region*
ET	*Equation of time*
K_V	Open-circuit voltage/temperature coefficient
K_I	Short circuit current/temperature coefficient

Greek Symbols

ρ	*Density*
η	*Efficiency*
K	*Boltzmann constant*
δ	*Declination angle*
θ	*Incident angle of solar radiation*
β	*Tilt angle of Solar panel (angle from horizontal surface to south) (slope)*
Φ	*Zenith angle*
Φ	*Azimuth angle*
L'	*Latitude angle*
H'	*Hour angle*

CHAPTER ONE

1. INTRODUCTION

In a world struggling with climate change and global warming, renewable sources of electricity generation are a very vital response to climate issues and also it is a key tool for developing countries, where a significant part of the population does not have access to the conventional electricity network. As per Trading Economics report [1], in Ethiopia electricity access is 42.9% of the population and according to World Bank collection of development indicators in 2016, in rural areas only 26.5% of the population have the access to electricity.

Using renewable energy, improved water supply and water resource management boosts countries economic growth and contributes greatly to eradicate poverty [2]. Resolving energy and water related challenges in water supply and sanitation system requires that, the costs for improved water supply and sanitation and energy and water resource management, be seen as sound public and private investment, and key strategy that boost economies, enable individuals and businesses to explore new income opportunities and provide a chance to grow [3].

As per UNESCO's GREET Program in 2012 report on Global Renewable Energy Education and Training Program [4], since water is a vital activity for the maintenance of humanity, the adoption of self-sustaining water pumping system practices using renewable energy resources becomes an essential part for the development of communities, either economically or socially.

Lots of new renewable energy conversion methods are explored in order to minimize dependence on conventional electricity and fossil fuels [3]. Consequently, the direct relationship between the availability of renewable resources and water demand of the society urges researchers and local stakeholders to analyze the feasibility of water pumping systems (WPS). The use of solar photovoltaic (PV) energy technology for WPS has been one of the most popular forms of solar energy application recently in remote areas, as well as in some urban areas [5]. However, the evaluation and analysis of availability of solar radiation and water resources before installing any PV system for the specific area is necessary in order to guarantee optimal solutions.

PV systems for water pumping developed around the world, and PV systems projects need some care and improvement as per the specific weather condition, the number of systems already installed shows that the technology is technically mature.

The main barriers to the implementation of PVWPS are related to technical aspects, and the sizing models of PVWPS are based on estimates of daily water consumption and static models (which is

not considering solar radiation and temperature of the specific area) and in economic aspects. The capital cost of PVWPS is still higher than the system driven by conventional electricity and diesel engine, while the operating cost are much lower and almost zero carbon emission and air pollution [5].

As challenges, it is necessary to adopt dynamic models design of PVWPS and policies that favor the mystification of the technology and that in a way the systems are financially viable, besides technical measures that collaborate for the best technical use of these systems.

In this thesis, a comprehensive review of different published scientific papers on the design and performance of solar photovoltaic energy for water pumping systems was revised in order to explore the best perspective of transition for the developing countries energy needs. The main objective of this thesis are modeling and analyzing hourly performance simulation of the solar powered water pumping system for Jigjiga in real weather conditions (real weather data collected from the agency for solar radiation and temperature), where Jigjiga is located in eastern part of Ethiopia indicated as the picture below at 9.38° N and 42.80° E.

Figure 1. 1 – Site Location Indication

In this thesis Jigjiga has been selected due to the potential for the solar radiation and ground water storage capacity. This encourage to analyze the PVPWP system performance using this solar energy potential and availability of the ground water in this area as research made by *Abeyou W. Worqlul* demonstrations.

1.1. Problem Statement

Water pumping system in Ethiopia use energy from conventional electricity network from EEP and diesel generators to pump water from moderate to deep groundwater and in surface water pumping to distribute and supply the water to the end users. Driving pumps using electricity from the grid and diesel generators have many draw backs and high running cost. There is a power shortage and interruption in the country and the diesel used to run the generator consume more cost, emit carbon to the atmosphere and highly pollutant to run pumps with a small amount of power input.

Therefore, due to energy related problems facing the pumping system, there is a high shortage of water in many urban and rural areas of Ethiopia. It is significant to find the solution for this water shortage to increase the life standard of the country, since the supply of electricity is very less. Using renewable energy is a feasible option to fulfill the energy need without affecting the life style of the population and environment. Hence, the aim of this thesis is to model efficient and effective PVPWPS, to solve the draw backs of conventional electricity and diesel generator, water pumping system and increase drinking water supply for small villages continuously without affecting the water pump throughout the day using hourly solar radiation and temperature data.

1.2. Objective

The general objective of this thesis is to model and analyze hourly performance simulation of solar powered water pumping system in the specific area Jigjiga in real weather conditions to determine the operating points and model the system, by taking hourly solar radiation and temperature data automatically measured in every 15 minute in Jigjiga.

1.3. Specific Objectives

The specific objective includes:

- ✓ Data sorting for the specified dates
- ✓ Compare measured global radiation and total radiation variation on optimally tilted panel
- ✓ Evaluate hourly variation of operating cell temperature

- ✓ Pump characteristic equation modeling
- ✓ Modeling the module and array
- ✓ Evaluate hourly variation of electrical characteristic output of the PV array
- ✓ Analyze hourly performance variation of the PVPWP system
- ✓ Evaluate efficiency of the system

1.4. Scope of the thesis

The scope of this thesis is to show hourly flow rate of water to the end user without interrupting the pumping system throughout the day as per the amount of power collected from solar radiation for 12 hours and supplied to the pump motor without using any power storage system. This means only storing the water in the reservoir pumped during the day time.

This thesis findings will benefit directly government, investor, and the end users by preventing unnecessary power shortage in water pumping system, by implementing renewable energy and improve water supply system problems faced by the end users. Using renewable energy in water facilities can produce a range of environmental, economic, and other benefits, including:

Reduce emission: using solar energy to run the pumps reduce carbon emission and clean environment for the residences.

Reduce energy costs: Local governments can achieve significant cost savings since the running cost for solar energy is almost zero comparing to electricity and fuel for diesel generators.

Saving energy and water security: Improving energy at a water facility reduces electricity demand, and helping to avoid the need to build new power plants. Efficient solar water pumping system strategies reduce the risk of water shortages, helping to ensure a reliable and continuous water supply.

Provide pure water availability: Improvements in renewable energy at water facilities can provide pure water availability for the resident and animals around the site.

1.5. Limitations

In this thesis, we intended to analyze the hourly performance simulation of solar powered water pumping system from ground water which is from moderate deep wells in Jigjiga area using submersible pumps. Metrological data and ground water level data of the specific area are the main input in order to simulate hourly performance of photovoltaic pumping system and determine the size of the PV and model the system by including MPPT control. The limitation to implement the system in any location is finding the real radiation and temperature data for the specific area.

1.6. Methodology

This section presents the methodology used to achieve objective of the thesis:

1.6.1. Data Collection

Data regarding solar radiation and temperature automatically registered using Pyranometer in every fifteen minutes throughout the days of the year was collected from Ethiopia National Meteorology Agency. Other primary data regarding to groundwater and background of water pumping system for Jigjiga area was collected from Ministry of Water, Irrigation and Electricity and different researches made in Ethiopia concerning to groundwater storage.

1.6.2. Determination, data analysis and system simulation

The raw data obtained are very bulky, therefore, sorting out the global radiation and temperature data and show the hourly availability of the solar radiation and temperature throughout a day are made for specific dates of the year to simplify the analysis. For the Assessment of Solar Energy Mstlab and theoretical methods are used to estimate the available solar energy incident on the PV array size. The optimization of the orientation angles, especially the tilt angle, was carried out to optimize the solar energy collected daily for a year.

Equipment (submersible pump and PV module with 6S x 4P configuration and MPPT control) has been selected and specified with its high performance, efficiency and data availability from the manufacturer, to model PVPWPS in the selected specific area.

Using SQF helical type submersible pump and the appropriate PV panel with a maximum power point tracking (MPPT) control, the modeling was evaluated for daily flow rate output performance under different power input that varies with daily solar radiation and temperature, different total dynamic head and performance efficiency of the pumping system, since, the water discharge from the well depends on the pump capacity and the available daily solar radiation of the area. Matlab algorism are used to simulate, data analysis of the given data, pump performance equation analysis, electrical characteristic curves of solar array and hourly flow rate performance simulation analysis of the system. At last the efficiency of the pumping system is evaluated.

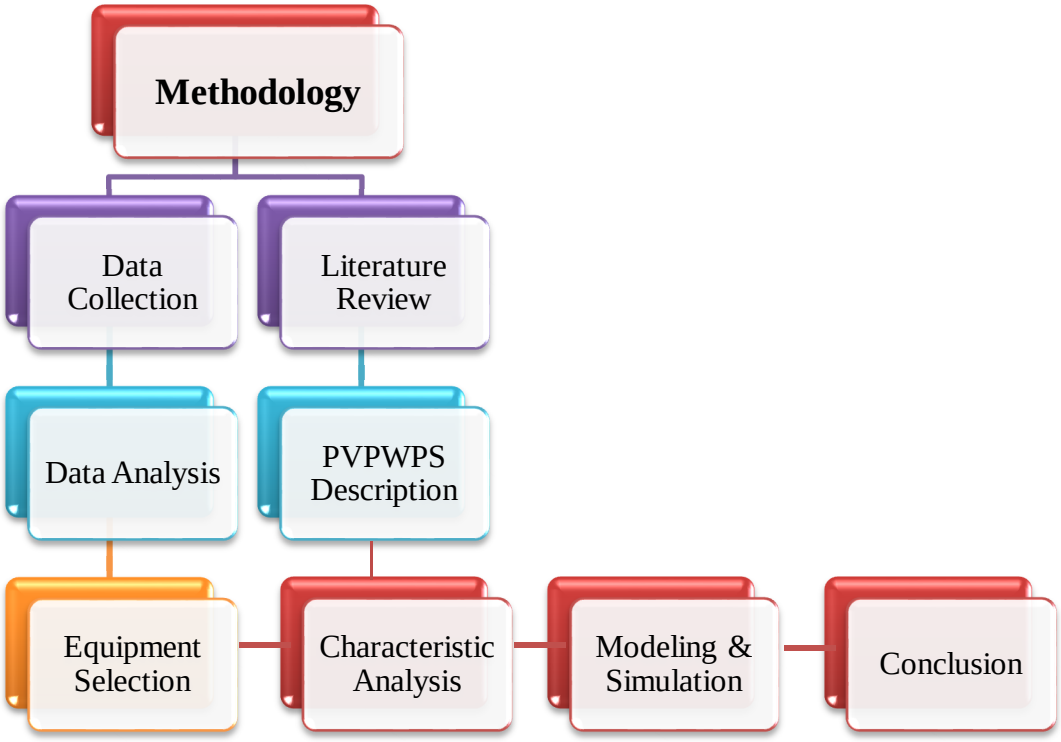

Figure 1. 2 - Flow Chart

1.7. Thesis structure

This section discuss the thesis structure followed to finalize. It is consists of seven chapters, bibliography, and appendix for additional information required. Chapter 1: provides an introduction to PVPWP system and energy system in Ethiopia. In this chapter problem statement, objective of the thesis, scope and methodology of the thesis are presented. In chapter 2: a detail literature of journal publications and different related papers are reviewed and presented. In chapter 3: a detail solar powered water pumping system are described and the specification of the equipment (pump and PV panel) are discussed. In chapter 4: PV device electrical characteristic modeling by different solar and PV system equations using the global radiation and temperature data (real weather data for Jigjiga). Chapter 5: discuss about curve and surface fitting by polynomial function to analyze manufacture data for the submersible pump. Chapter 6: are result and discussion of the thesis. In this chapter results on data analysis, data sorting, comparing the measured global radiation on horizontal plane to the total radiation variation on optimally tilted panel, pump characteristic equation using polynomial function, simulation results of PV module and array, hourly variation of electrical characteristic output of the PV array and hourly performance variation of the PVPWP system are presented. Finally in chapter 7: conclusion and recommendation for future work are presented and followed by bibliography and appendix.

CHAPTER TWO

2. LITERATURE REVIEW

A comprehensive, detailed literature reviews here conducted to identify alternative renewable energy tools, practices, processes, and technologies associated with the implementation of the solar PV powered water pumping system, which is very supportive to model and use the advanced technologies in PVPWPS. The reviewed researches included solar pumping system performance simulation analysis and experimental analysis associated with PV panel handling, conservation practices, alternative energy generating, and solar pumping mechanisms to mitigate community problems in water supply.

The mandatory data collection as well as appropriate information necessary to analyze this PVPWPS are identified. This thesis included review of academic researches, numerous solar PV industry publications, pertinent PV Research Foundation reports, presentations on renewable energy conferences, and Web sites of energy and water pumping related organizations and associations.

Abdulbasit Nasir [6] in 2016, study Design, Simulation and Analysis of Photovoltaic Water Pumping System for Irrigation of a Potato Farm at Gerenbo southern Ethiopia, aiming to present the benefits of replacing diesel water pumping system by photovoltaic water pumping system in irrigation of a potato farm using river (surface) water available in the area. The finding of this research shows us using solar power for the water pumping system is a good opportunity interms of solar availability, carbon emission control and economically effective.

Mya Su Kyi, Lu Maw, Hla Myo Tun [7] in 2016, study of Solar PV Sizing of Water Pumping System for Irrigation of Asparagus, aiming to supply water for the irrigation farm fields in alternative way by generating electricity through solar panels mainly consists of two modules, solar pumping module and automatic irrigation module. The finding of the research paper shows the model always ensured the sufficient level of water in the Asparagus field and avoiding the under irrigation and over irrigation, also using this system, one can serve manpower, water to get better manufacture and eventually income for the individuals using this system. In this research paper one can understand they briefly discuss the alternative used to generate power through PV panel and supply the sufficient water capacity as required in the field

Shatadru Biswas and M. Tariq Iqbal [8] in 2018, study Dynamic Modelling of a Solar Water Pumping System with Energy Storage, aiming to observe the response in pump speed and bus

voltage with the change in irradiance and temperature built in MATLAB/SIMULINK environment for both battery-less and battery-based system to run a motor-pump set using solar energy to lift ground water for irrigation purpose. The finding of this research shows that the solar water pumping system can be integrated to irrigation systems in Bangladesh as it is feasible solution for longer period and economically feasible solution to meet the irrigation challenges faced during dry season in that area and can improve the life standard.

A. Allouhi, M.S. Buker, H. El-houari, A. Boharb, M. Benzakour Amine, T. Kousksou, A. Jamil [9] in 2018, study PV water pumping systems for domestic uses in remote areas: Sizing process, simulation and economic evaluation, aiming to examine an optimum PV system configuration that is capable of supplying a solar submersible pump system to fulfill domestic water needs of five isolated houses located in a Moroccan remote area. Using a detailed approach for the design of an optimized PV water pumping system based on real water usage data, system design work and performance assessment based on hourly climatic conditions. The conclusion of this paper work shows that, two positive displacement pumps of 140W connected in parallel and storage tank of $24m^3$ could achieve the design requirements and by comparing two different PVWP configurations, direct coupling and MPPT DC converter, this research shows MPPT DC configuration has it nearly 25% higher than that of the direct coupling system and reduce PV module capacity install by 30%.

Mansur Aliyu, Ghassan Hassan, Syed A. Said, Muhammad U. Siddiqui, Ali T. Alawami, Ibrahim M. Elamin [10] in 2018, study a review of solar-powered water pumping systems comparing to Diesel-powered pumping system in different countries. The result of this research paper shows, almost all the installed solar-powered water pumping systems heads do not exceed 200 m, since as increase in system head there is increase in power supply, and this systems are more economical at low pumping capacities compared to diesel and wind-powered water pumping systems. A solar-powered water pumping systems contributes to a clean environment by reducing the carbon emission compared to other power supply system.

S.S. Chandel, M.Nagaraju Naik, Rahul Chandel [11] in 2015, doing a research on a Review of solar photovoltaic water pumping system technology for irrigation and community drinking water supplies, studying current state of water pumping technology and performance parameter, economic and environmental aspect of the system. In their conclusion, PV water pumping technology is reliable and economically viable alternative for both electric and diesel power supply in water pumping system, best option for remote inaccessible locations with no grid and recommended

further research on factors affecting the efficiency and system performance improving techniques, like further analysis on modeling the pumping system in real weather conditions.

S.S. Chandel, M.Nagaraju Naik, Rahul Chandel [12] in 2017, do their research paper on a Review of performance studies of direct coupled photovoltaic water pumping systems and case study along with old functional solar pump in a western Indian Himalayan location. The result of this research paper shows that, the difference between measured and PV Syst simulated pump efficiency and overall PV system efficiency are 4.84% and 2.2% respectively. The performance results shows that the system is capable of pumping at an average of 829 l/h. The rated power output of the PV modules used in the system is 396Wp which has been reduced to 235 Wp. The total average power generated by PV array during the observation period is 95.56 W which is quite less to obtain the nominal flow rate of the pump. The power generated by the PV modules is reduced due to degradation of PV modules used in the system due to prolonged 28 years of field exposure.

Mr. Malla.Jagan Mohana Rao, Dr. Manoj Kumar Sahu, Dr. Pravat Kumar Subudhi [13] in 2018, study PV based water pumping system for agricultural sector aiming to evaluate ways of efficient PV powered water pumping system. Photovoltaic-battery hybrid system feds the vector control of an asynchronous motor, PV generator, converter of DC-DC, battery, converter of DC-AC, an induction motor controlled by a vector and the centrifugal pump are investigated in this paper.

The result is presented based on Matlab/Simulink analysis considering head as 25 m and maximum water discharge as 300 gal/min, induction motor of rating 5 hp (3.7 kW) is considered to be connected at AC bus. PV array is considered of rating 4.7 kW which is the combination of 22 solar modules in series. Each module having open circuit voltage as 36.90 V, short circuit current is 8.01A, voltage at maximum power (V_{mpp}) is 30.3V and current at maximum power (I_{mpp}) is 7.10. The simulation results are discussed by considering maximum power point tracking, change in solar irradiance, no irradiance or non-sunny days and intermittent changes in solar irradiance.

Arunendra K. Tiwari, Vilas R. Kalamkar, [14] in 2018, study the effects of total head and solar radiation on the performance of solar water pumping system and analyzed with the optimized PV array configuration. Four pumping head have been analyzed (4 bar, 6 bar, 8 bar and 10 bar). The experiments have been performed for various heads on clear sunny daylight hours in an artificial well at VNIT campus Nagpur (India). The effect of variation of radiation on the performance of pump has also been studied. The best system efficiency is founded for the total head of 10 bar which is suggested for helical rotor submersible pump. Also, for Nagpur (India), the system should be sized

as per the irradiance range 400 to 800 W/m2, as more than 60 % of the total solar energy falls in this range.

The SPVWPS with a two axis manual tracking is installed at the outdoor PV research facility at the rooftop. The directly coupled SPVWPS comprised of:

- Photovoltaic array 1.6 kW: each panel of 200 W connected in optimized configurations.
- Grundfos submersible pump (model SQF) with helical rotor.
- MSF 3 motor (2 hp) with Maximum Power Point Tracking (MPPT).

The result of the experimental analysis at real condition of the specific site shows, the radiation available at a site affects the pump output for different operational head, at higher radiation the flow rate remains almost constant as in the present case at 800 W/m^2 but the flow rate deviates significantly (43.5%), at low radiation for different heads.

M. Benghanem, K.O. Daffallah, A. Almohammedi [15] in 2018, study the Estimation of daily flow rate of photovoltaic water pumping systems using solar radiation data, aiming to develop a general method for the evaluation of the long term performance of a direct coupled photovoltaic powered water pumping system and simulate the flow rate Q by using only the solar radiation data. The nonlinear relation between water flow rate and solar power obtained experimentally and then used for performance prediction. The model proposed enables to simulate the water flow rate using solar radiation data for different heads (50 m, 60 m, 70 m and 80 m) and for 8S x 3P PV array configuration. The experimental data are obtained from pumping test facility located at Madinah site (Saudi Arabia). The performances are calculated using the measured solar radiation data of different locations in Saudi Arabia. Knowing the solar radiation data, they estimate with a good precision the water flow rate Q in five locations (Al-Jouf, Solar Village, AL Ahsa, Madinah and Gizan) in Saudi Arabia. The flow rate Q increases with the increase of pump power for different heads following the nonlinear model proposed.

Bahadur Singh Pali, Shelly Vadhera [16] in 2019, study a novel solar photovoltaic system with pumped-water storage for continuous power at constant voltage. The proposed system comprises of a solar photovoltaic (SPV) system, solar water pump, pico-hydro turbine-generator and pumped-hydro energy storage system without use of batteries, inverter, transformer, and charging or controlling circuits. The main constituents of the present SPV-PHES system are the SPV array, SWP, PHT open well and the UR. Therefore, the complete model of the proposed system comprises of its constituents modelling. Mathematical model presented and is carried out in Matlab using real

solar irradiation data for 72 hours. The result of this paper shows, the daily maximum fall in voltage during the period of 14 h (5 PM to 7 AM) is 1.4%, 3.2% and 3.2% for 3 consecutive days respectively. Here, it is observed that the voltage fall on second day is equal to that of third day, which shows that there is no drop in voltage after second day. This observation assures that the present system is stable and capable for continuous operation up to the desired period without any further fall in voltage, but they didn't consider the economical aspect and the system is expensive.

Essam E. Aboul Zahab, Aziza M. Zaki, Mohamed M. El-sotouhy [17] in 2017, this research paper discuss on design and control of a standalone PV water pumping system. Photovoltaic (PV) is the main power source, and lead acid batteries are used as energy storage system, to supply a water pump driven by a brushless direct current (BLDC) motor. The proposed control strategy consists of three control units. The first unit is to control the speed and hysteresis current controller for BLDC motor. The maximum power point tracking (MPPT) is the second control unit, and the battery charging/discharging system is controlled by the third controller. The standalone PV water pumping system used is consists of a PV array, a maximum power point tracking (MPPT) system controlling a DC–DC boost converter which drives a BLDC motor driving a positive displacement water pump. Two MPPT techniques are introduced perturb and observe (P&O) method and fuzzy logic control (FLC) method, and the two methods are compared. The simulation result shows, FLC is faster and has lower oscillation around the maximum power point than the P&O. The battery backing system is also designed together with its control system to satisfy system requirements all the time.

M. Benghanem, K.O. Daffallah, S.N. Alamri, A.A. Joraid [18] in 2014, in their research they study Effect of pumping head on solar water pumping system. The aim of this work is to determine the effect of pumping head on PVWPS using the optimum PV array configuration, adequate to supply a DC Helical pump with an optimum energy amount, under the outdoor conditions of Madinah site. Four different pumping head have been tested (50 m, 60 m, 70 m and 80 m). The tests have been carried for a different heads, under sunny daylight hours, in a real well at a farm in Madinah site. The flow rate Q depends basically on two factors: the pumping head H and the global solar irradiation Hg.

The result of this paper shows that system efficiency increases with increasing solar radiation until the pump reached their maximum power. Also, system efficiency increases with decreasing pumping head during low solar radiation. During the maximum power (high solar radiation), they found that the optimum pumping head correspond to the best average system efficiency which is obtained for the head of 80 m. This head is considered as the optimal pumping head profile for the considered PV

pumping system. Also, increasing PV array size generally increases flow rate and system efficiency since it increases the power input to the system.

M. Benghanem, K.O. Daffallah, A.A. Joraid, S.N. Alamri, A. Jaber [19] in 2013, study performances of solar water pumping system using helical pump for a deep well: a case study for Madinah, Saudi Arabia. Which is an experimental analysis, aiming to determine an optimum photovoltaic (PV) array configuration, adequate to supply a DC Helical pump with an optimum energy amount, under the outdoor conditions of Madinah site. They test four different PV array configurations (6S _ 3P, 6S _ 4P, 8S _ 3P and 12S _ 2P). The tests they have been carried was for a head of 80 m, under sunny daylight hours, in a real well at a farm in Madinah site. The system components are:

- Submersible pump.
- Solar panels.

By setting a PV water pumping system (PVWPS) in a reel well of 80 m of head and using the components of the PVWPS composed of: photovoltaic generator of 1.8 KW, submersible helical pump, flow meter of type Electromagnetic and Agilent data logger system connected to computer for data acquisition and treatment, they obtain a best result for two PV array configurations (6S _ 4P) and (8S _ 3P), which are suitable to provide the optimum energy in their case. Powered by the selected PV array configurations, the helical submersible pump delivered a maximum daily average volume of water needed a day, which is (22 m^3/day) in their case.

A. Allouhi, M.S. Buker, H. El-houari, A. Boharb, M. Benzakour Amine, T. Kousksou, A. Jamil [20] in 2019, study a PV water pumping systems for domestic uses in remote areas: Sizing process, simulation and economic evaluation. The aim of this work is to examine an optimum PV system configuration that is capable of supplying a solar submersible pump system to fulfill domestic water needs of five isolated houses located in a Moroccan remote area. A detailed approach for the design of an optimized PV water pumping system based on real water usage data is proposed. Besides, system design work and performance assessment were carried out based on hourly climatic conditions. Overall, two approaches were investigated for an optimum design of the proposed system. Annual simulations indicated that the direct coupling, as a first option, appears to be unfitting configuration for water pumping in this case.

The result [20] shows, a residential water use survey conducted for 30 months shows that the average water demand did not exceed 6m^3 per day for the targeted project. Based on the site's

general characteristics and considering four days of autonomy, it was found that two positive displacement pumps of 140W connected in parallel and storage tank of 24m^3 could achieve the design requirements. Comparing the direct coupled and MPPT control, applying the MPPT DC approach to the PVWP system yields a reduction in the required capacity of PV modules (from 480 Wp to 320 Wp). This implies a reduction of nearly 30% in the PV module capacity to install and therefore improve the economic feasibility of PVWP substantially.

The above literatures shows different models on design of PVPWPS, technology advancement of the system, carbon emission and pollution control from using renewable energy, economic and social aspects, the difference b/n using direct coupled and MPPT control in PV panel and the advantage of MPPT in PV powered water pumping system, experimental results in optimum PV panel configurations, TDH effect in pumping system, the idea of using water storage instead of using solar batteries (which store water not energy), the effect of the variation of solar radiation on the efficiency of the pumping system, experimental analysis in different TDH of the system, etc., which is the gap during modeling and implementation of PV powered water pumping system and a very important points to analyze and model the appropriate PVPWP system in real weather condition of specific locations.

CHAPTER THREE

3. PV POWERED WATER PUMPING SYSTEM

3.1. Pumping System Description

The volume of water pumped by a solar-powered system in a given interval depends on the total amount of solar energy available in that time period. The flow rate capacity of the water pumped is determined by both the intensity of the solar energy available and the size of the PV array [5]. Solar PV technology applied to WPS is based on conversion of solar energy into electrical energy by solar panels to power a water pump motor. PV panels are connected to a DC or AC motor, which converts the electrical energy received from the panels into mechanical energy, and is subsequently converted into hydraulic energy. The hydraulic power of the pump allows to store water in the reservoir [5].

PVWPS generally consist of:

- An area of PV modules mounted on a structure with fixed arrangement or manual/automatic tracking,
- Pumping system (motor-pump), which can be surface mounted, submersible or floating, (in this case which is a deep well submersible pump)
- Power conditioning system, which generally consists of converter, inverter, controller, etc.,
- Water storage system, sensors.

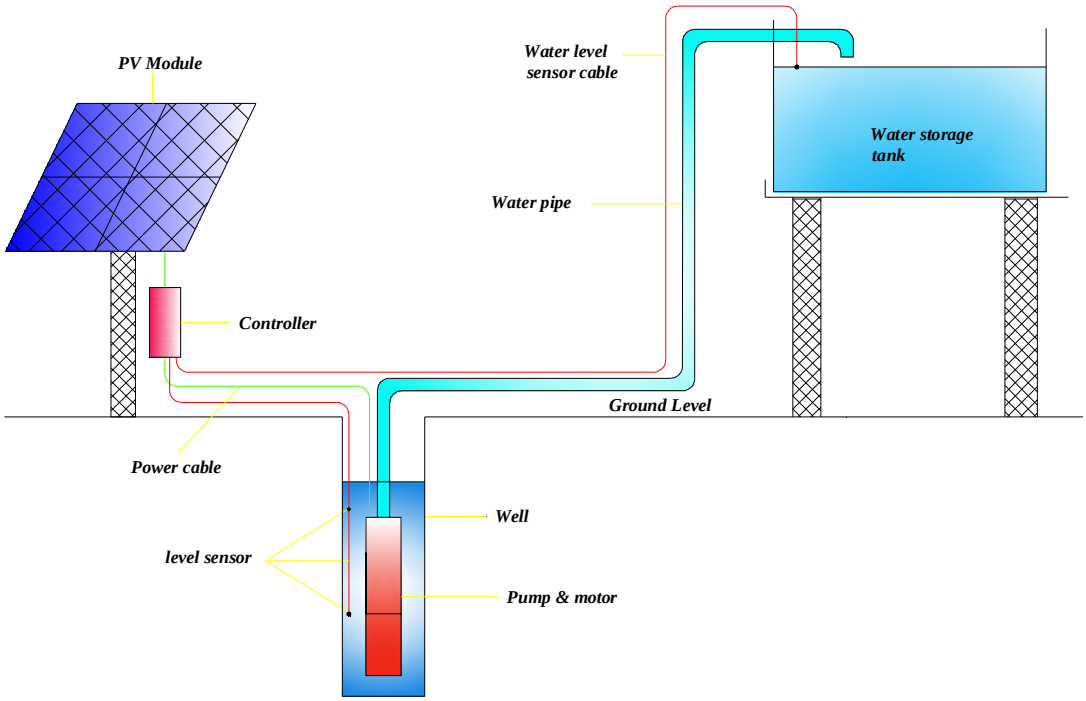

Figure 3. 1 - Schematic Diagram of PVPWP System

3.2. Background and Technological Advancement

Solar PV technology for water pumping has been explored over 5 centuries ago. The conversion of solar energy into mechanical or electrical energy for water pumping is used since the 15th century, although the first reported PVWPS was installed in the Soviet Union only in 1964. The maximum power of the PV system installed at that time, to activate the water pump, was 373 W which developed in France [21].

Initially, solar pumping systems with direct coupling with the water pumps were introduced; however, they presented limitations in the performance of the system, by not operating at the maximum power point of the PV generator. Despite this disadvantage, this type of system is considered to be simple and reliable [22], being also efficient for use in small irrigations system since it is economically feasible [23]. In the last decade, these systems have been improving in its performance due to the addition of the maximum power point tracker (MPPT) control systems [24].

The first generation of PVWPS was characterized by the use of centrifugal pumps driven by direct current (DC) motors and variable frequency alternating current (AC) motors, whose hydraulic efficiency ranges from 25% to 35%. The second generation of PVWPS considered positive displacement pumps, characterized by low photovoltaic power (100 Wp to 400 Wp) input, low capital cost and hydraulic efficiencies up to 70% [25]. Currently, PVWPS of the first and second generation are equipped with electronic control systems, pump speed and maximum power trackers, to increase the overall system performance [11], whose hydraulic efficiencies reach values of 92%.

In general, as solar energy vision in Ethiopia opportunities for creating a PV industry magazine, Ethiopia receive 5000-7000 Wh/m^2 solar irradiance according to season and region. The average solar radiation is more or less uniform, which is around 5.2 $kwh/m^2/day$ [26]. This value vary seasonally and locations. Figure 3.2 shows solar irradiation of the country in $kwh/m^2/day$.

The coverage of electricity in Ethiopia around 86% is from hydropower's [26]. Solar PV are being promoted to replace fuel based power generation and off-grid electrical needs. Ethiopia is thought to have about 5 MW of off-grid solar. Almost all current solar power is used for telecommunications and other uses include village well pumps, health care and school lighting. Government has been developing initiative plant to bring solar power to 150,000 households by 2015, the phase included 1MW of panels [27]. The first large installation of solar was a village grid of 10 kW in 1985 expanded to 30 kW in 1989.

As per new PV panel plant commissioned in Ethiopia on PV Magazine report, a solar panel assembly plant opened in Addis Ababa in early 2013 capable of making 20 MW of panel per year. Ethiopian Electric Power (EEP) plan to implement 500MW solar power plant [26]. This shows the concern of the government to use renewable energy available in the country and encourage individuals to be engaged in this system.

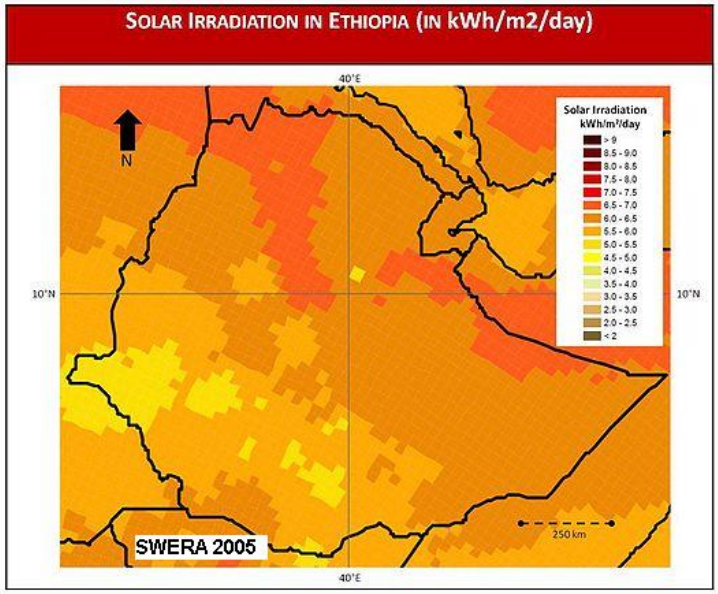

Figure 3. 2 - Ethiopia Solar Irradiation in KWH/m^2/Day

Abeyou W. Worqlul, [28] in their assessment of potential land suitable for surface irrigation using groundwater in Ethiopia, presents the total groundwater storage of Ethiopia as shown in the Figure 3.3 below.

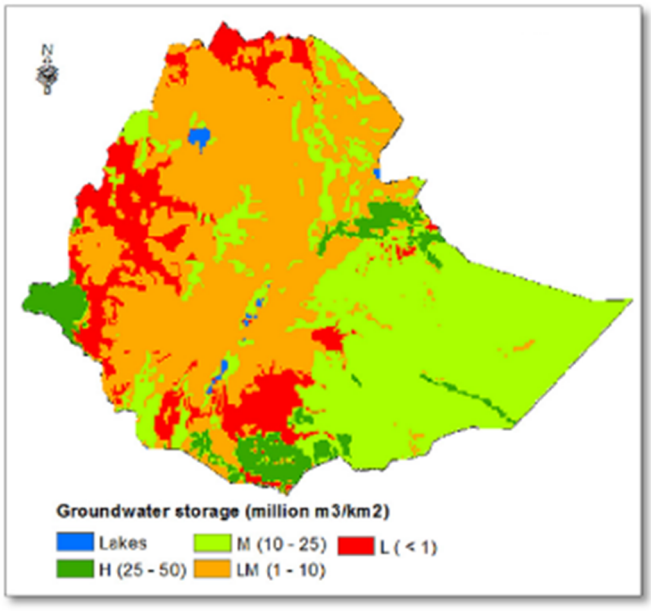

Figure 3. 3 - Ground Water Storage in Ethiopia

The above two Figures (Figure 3.2 and Figure 3.3) shows the solar potential and ground water storage around the country, this will inspire to implement a PV system using this solar energy in any sectors and to model and evaluate performance simulation of PV powered water pumping system, in our case of Jigjiga real weather conditions, which is solar radiation and temperature using previous years data.

3.3. Photovoltaic Water Pumping Systems Parameters

The use of solar photovoltaic (PV) energy technology for water pumping systems (WPS) has been one of the most popular forms of solar energy application recently in remote areas, as well as in some urban areas with limited access to conventional electricity and deiseal [5].

In this order it is necessary to define the parameters of the system, even if it is by estimation. Thus, the selection of a pump for PVWPS depends on the following variables that affect the performance of the system and overall system efficiency [29].

Solar resource:

- Solar radiation availability,
- Ambient temperature at the location.

Water:

- Groundwater capacity to be pumped,
- Flow rate of water, which is influenced by weather conditions at the location, especially solar irradiance and air temperature variations,
- Size of water storage tank or reservoir which depends on water to be pumped per day.

Total Dynamic Head (TDH):

- Discharge head (height from pump to storage inlet), and
- Frictional losses.

PV system:

- PV array energy (kWh) and Power (kw),
- P-V, P-I, I-V, R-V of the PV array (electric characteristics of the PV array)
- MPPT control
- Efficiency of PV technology used.

Pump & motor:

- Pump power (kw),
- H vs Q curves and operating point of the pump
- Pump efficiency (%).

The modeling and performance analysis of a PVWPS generally consists in determining the size of a system that will meet the needs of the user with minimum total investment costs, taking into account technical, economic and social issues, specific to each project. Although, the use of simulation programs allows solving problems of performance optimization PV systems, there are other identified methods such as: intuitive, numerical, analytical and intelligent techniques [30].

Thus, the respective design procedures can be presented in the process flow procedure shown in Figure 3.4 below.

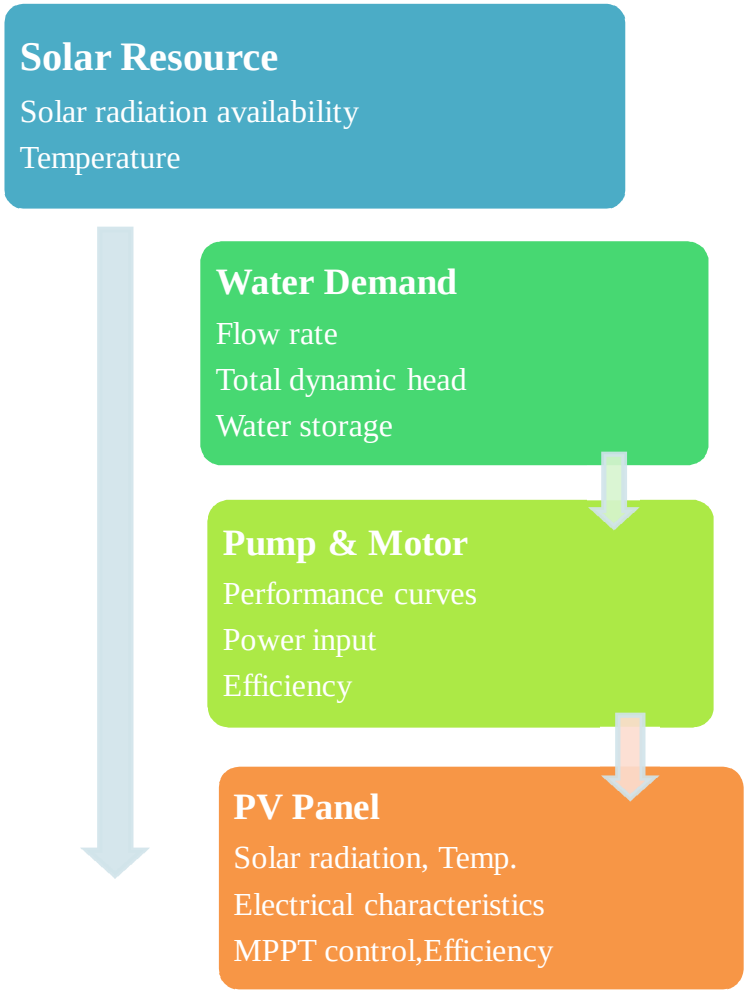

Figure 3. 4 - PVWPS Simulation Modeling Procedures

3.4. Solar Radiation Measurement

Solar energy is the primary source of all energy sources. Solar radiation reaching the Earth's atmosphere can be decomposed in different ways for analysis purposes [31]. For PV utilization, the most interesting is horizontal global irradiance, which quantifies the irradiance received by a flat horizontal surface [W/m^2]. It is composed of horizontal diffuse irradiance and direct normal irradiance.

The solar radiation is usually measured with the help of a Pyranometer that measures the global radiation, while direct radiation can be obtained with a Pyrheliometer. The diffuse radiation can be determined by subtracting the measured direct radiation from the global radiation [31] as briefly described in the next chapter 4. Solar radiation and temperature data are obtained from Ethiopian National Metrology, which is the main input for this modeling.

The local measurement at Jigjiga is made every 15 minutes of the day using Pyranometer SP-Lite and CMP3, solar radiation in (W/m^2) and temperature in (^oC). The measured data taken from the national meteorology is for 9 years (from 2011 – 2019) in every 15 minutes, which means 96 radiation and temperature data for every days of a year measure automatically. Data resulting from measurements are reduced to specific year values and seasonal variability for a year to simplify the data analysis, and to model and analyze the hourly performance simulation of PVPWP system.

3.5. Determination of Hydraulic power

For determination of water demand, it is necessary to consider the final use of water and/or user requirements. In this case, the aim is to supply the drinking water to the community in small scale (human consumption in litters/day). For cases in which an exact value of water consumption is not available, Table 3.1 provides results illustrating water consumption information by some activities.

Table 3. 1: Estimated average consumption of water by end use, in liters [29].

Human Consumption	Litter/person. day	Animal Consumption	Litter/animal. day	Cultivation	Litter/ha. day
Survival	5	Cattle (milk)	70	Vegetable garden for subsistence	25,000
Large urban center	10-100	Cattle (cutting)	40	Tomato	46,200
Small farms	40-70	Sheep/goat	5	Corn (Maize)	50,000
-	-	Swine	15	Been	48,000

Hydraulic power, P_H (KW), required to supply a water flow rate (Q) at a certain TDH, considering the end use of the water and/or user requirements is given by Equation (3.1) [32]:

$$\boldsymbol{P_H = Q.TDH.\rho.g.\eta_{pm}} \quad (3.1)$$

Where:

- Q - water flow rate (m^3/h);
- TDH - total dynamic head (m);

- ρ - water density (1000 kg/m^3 at 0^0C and 1 bar);
- g - gravity (9.81 m/s^2).

In order to calculate the total head, the pressure head must be considered and suction head is neglected since submersible pumps are used in this case. Where significant, the pressure drop in piping and pipe connections (elbow) are taken into account on this PVPWPS modeling. Usually these loss coefficients are given by the pipe manufacturers and connections.

However, if the hydraulic power varies from day to day or month to month, etc., due to varying of solar radiation and water available in ground, the PVWPS should be designed for the worst-case combination of solar radiation energy and water demand [33].

It is often useful to determine whether a given pipe flow is laminar or turbulent. This is necessary, because different methods of analysis or different equations are sometimes needed for the two different flow regimes[34].

Laminar flow takes place for flow situations with low fluid velocity and high fluid viscosity. In laminar flow, all of the fluid velocity vectors line up in the direction of flow. Turbulent flow, on the other hand, is characterized by turbulence and mixing in the flow. It has point velocity vectors in all directions, but the overall flow is in one direction. Turbulent flow takes place in flow situations with high fluid velocity and low fluid viscosity[34].

As the classic experiments of Osborne Reynolds, in which he injected dye into fluids flowing under a variety of conditions and identified the group of parameters now known as the Reynolds Number for determining whether pipe flow will be laminar or turbulent. He observed that under laminar flow conditions, the dye flows in a streamline and doesn't mix into the rest of the flowing fluid. Under turbulent flow conditions, the turbulence mixes dye into all of the flowing fluid. Based on Reynolds' experiments and subsequent measurements, the criteria now in widespread use is that pipe flow will be laminar for a Reynolds Number (Re) less than 2100 and it will be turbulent for a Re greater than 4000. For $2100 < Re < 4000$, [34] called the transition region, the flow may be either laminar or turbulent, depending upon factors like the entrance conditions into the pipe and the roughness of the pipe surface.

Straight Pipe Head Loss

Calculation of the frictional head loss for a specified flow rate of a given fluid at a given temperature through a pipe of known diameter, length, and material. can be done using the Darcy Weisbach equation [34].

$$h_L = f\left(\frac{L}{D}\right)\left(\frac{V^2}{2g}\right) \quad (3.2)$$

The step-by-step process for this calculation is as follows:

- Determine the density and viscosity of the flowing fluid at the specified temperature
- Calculate the fluid velocity from $\left(V = \frac{Q}{A} = \frac{Q}{\frac{\pi D^2}{4}}\right)$
- Calculate the Reynolds Number $\left(Re = \frac{DV\rho}{\mu}\right)$, where μ is viscosity and ρ is density of water
- Find the pipe roughness value (ε) for the specified pipe material.
- Calculate the pipe roughness ratio, $\left(\varepsilon/_D\right)$.
- Determine the Moody friction factor value using the Moody diagram and/or friction factor equation(s), with the calculated values of (Re) and$\left(\varepsilon/_D\right)$.
- Calculate the frictional head loss using the Darcy Weisbach equation and the specified or calculated values of L, D, and V.

Minor Head Losses

As Harlan H. Bengtson [34], the term "minor losses" refers to head loss or pressure drop due to flow through pipe fittings (e.g. valves, elbows, or tees), entrances and exits, changes in pipe diameter, and any other causes of head loss besides the straight pipe portion of the flow.

The general equation for calculating the minor loss of a fitting in a pipe system is:

$$h_L = K\left(\frac{V^2}{2g}\right) \quad (3.3)$$

Where **K** is the minor loss coefficient for the particular fitting. For several fittings in a pipe system, all of the **K** values can be summed to give; $h_L = \sum K\left(\frac{V^2}{2g}\right)$. Values of **K** for fittings, changes in cross-section, etc. where; $= Q/A = Q/\pi D^2/4$.

Determination of the electric power needs

The electric power to the input of the motor-pump unit, P_{EL} (kw), is given by Equation (3.4) [32]:

$$P_{EL} = \frac{P_H}{\eta_{pm}} \quad (3.4)$$

Where: η_{pm} - Efficiency of the motor pump unit.

Electricity power consumption is a multiplication of current (I) and voltage (V)

Hence: $P_{con} = V \times I$

Determination of the photovoltaic power needs

A simplified method proposes a simple arithmetic formula that can be used to determine the approximate value of the rated power of the Photovoltaic panel according to Equation (3.5) [32]:

$$P_{PV} = \frac{P_{EL} x\, G_{REF}}{G_{Glob} x F_Q} \quad (3.5)$$

Where:

- P_{PV} - peak power of the PV array under Standard Test Conditions (STC: radiance = 1000 W/m^2, AM 1.5, cell temperature = 25^{0}C) [kw],
- G_{GLOB} - global solar radiance on a horizontal surface [kw/m^2],
- G_{REF} - incident solar radiance at STC [1 kw/m^2],
- F_Q - quality factor of the system.

To obtain the PV system efficiency is used Equation (3.6):

$$\eta_{PV} = \frac{P_{PV}}{G_{Glob} x A_{Array}} x100 \quad (3.6)$$

Where:

- A_{array} - area of the PV array [m^2].

The overall solar water pump system efficiency is obtained by Equation (3.7) [32]:

$$\eta_{total} = \eta_{PV} x \eta_{PM} \quad (3.7)$$

3.6. MPPT Control

In a (Power-Voltage or current-voltage) curve of a solar panel, there is an optimum operating point such that the PV delivers the maximum possible power to the load. This unique point is the maximum power point (MPP) of solar panel[24].

Because of the photovoltaic nature of solar panels, their current-voltage, or IV, curves depend on temperature and irradiance levels. Therefore, the operating current and voltage which maximize power output will change with environmental conditions. As the optimum point changes with the natural conditions so it is very important to track the maximum power point (MPP) for a successful PV system. So in PV systems a maximum power point tracker (MPPT) is very much needed. In most PV systems a control algorithm, namely maximum power point tracking algorithm is utilized to have the full advantage of the PV systems[17].

For any given set of operational conditions, cells have a single operating point where the values of the current (I) and voltage (V) of the cell result in a maximum power output. These values correspond to a particular load resistance, R= V/I, as specified by Ohm's Law[24]. The power P is given by P = V*I. From basic circuit theory, the power delivered from or to a device is optimized where the derivative of the I-V curve is equal and opposite the I/V ratio. This is known as the maximum power point (MPP) and corresponds to the "knee" of the curve. The load with resistance R=V/I, which is equal to the reciprocal of this value and draws the maximum power from the device

is sometimes called the characteristic resistance of the cell. This is a dynamic quantity which changes depending on the level of illumination, as well as other factors such as temperature and the age of the cell. If the resistance is lower or higher than this value, the power drawn will be less than the maximum available, and thus the cell will not be used as efficiently as it could be. Maximum power point trackers utilize different types of control circuit or logic to search for this point and thus to allow the converter circuit to extract the maximum power available from a cell [17].

There are many different approaches to maximizing the power from a PV system, this range from using simple voltage relationships to more complexes multiple sample based analysis.
There are conventional methods for MPPT like: Constant Voltage method, Open Circuit Voltage method, Short Circuit Current method, Perturb and Observe method, Incremental Conductance method, Temperature method, Temperature Parametric method [20].

In this thesis a constant voltage method MPPT control is used since, the constant voltage method is the simplest method. This method simply uses single voltage to represent the V_{mp}. In some cases this value is programmed by an external resistor connected to a current source pin of the control IC. In this case, this resistor can be part of a network that includes a NTC thermistor so the value can be temperature 25 degree compensated [17]. For the various different irradiance variations, the method will collect about 80% of the available maximum power. The actual performance will be determined by the average level of irradiance. In the cases of low levels of irradiance the results can be better.

3.7. Solar PV Powered Pump Selection

Most pumps used for water supply system are of the helical or centrifugal type driven by electric motors or diesel driven. They have complex and unique head/flow characteristics and associated energy efficiency curves. Every pump is designed and manufactured to operate most efficiently at a specific duty point. The duty point is the point at which the pump produces the required flow (Q) at the required head (H) which it has to overcome [35].

In this thesis a deep well submersible pump is required to model the system. There is two types of pump used to withdraw water from the ground. Which is centrifugal type deep well submersible pump integrated with induction motor in fixed speed type or controlled by variable speed drive (which is an electronic device that control the frequency input to the induction motor, then increase or decrease the motor speed, in consequence vary the output flowrate of the pump as per the power input to the system) with small variation of frequency or speed the flowrate varies significantly and its suitable for large flowrate pumping system. The other one is helical type deep well submersible

pump integrated with permanent magnet motor which the speed varied from 500 – 3600 rpm as per the power input to the system (and advanced technology and more efficient that induction motors which uses permanent magnet rather than windings). Helical type submersible pumps are for high head and for small flowrate. In this thesis helical type submersible pump is selected since, the total dynamic head is high and the required flowrate amount is small.

In this thesis solar powered helical SQF type submersible pump was selected for the model and performance simulation of PVPWP system in a real weather condition according to manufacturer specification and the overall efficiency of the pump and motor speed variation, since the power input to the system varies as per the solar radiation and temperature variation of the specific location.

Pump performance character is subject to fixed and transient head/pressures that the pump encounters in the pumping pipe network in which it operates [35]. The analysis of pump performance and operational outcomes is undertaken by utilizing pump characteristic curves. These curves are generated by pump manufacturers for each specific pump type.

3.8. Pump Specification

As per the manufacturer the SQFlex system is a reliable water supply system based on renewable energy sources, such as solar and wind energy. The SQFlex system incorporates an SQF submersible pump. Very flexible as to its energy supply and performance, the SQFlex system can be combined and adapted to any need according to the conditions on the installation site. This system is suitable for water supply applications in remote locations.

The system components are: SQF submersible pump, control unit, switch box, breaker box, MPPT controller and solar panels. The SQF pump range comprises two pump technologies:

• Helical rotor pump (3") for high heads and small flow rates

• Centrifugal pump (4") for low heads and large flow rates.

The motor is designed according to the permanent-magnet principle with built-in electronic unit since, permanent magnet DC motors are more efficient than traditional induction motors. The SQFlex 3" motor range comprises only one motor size, the MSF 3 with a maximum power input (P_1) of 1400 W. The motor speed range is 500-3600 rpm, depending on power input and load. The motor has three internal limitations: maximum power input (P1) of 1400 W, maximum current of 8.4 A, maximum speed of 3600 rpm.

The pump delivers its maximum performance when one of the above limitations is reached. The motor can be supplied with either DC or AC voltage: 30-300 VDC, PE, and 1 x 90-240 V - 10 %/+ 6 %, 50/60 Hz, PE. The solar modules are equipped with plugs and sockets enabling easy connection in series and in parallel.

The 3" SQFlex pump with helical rotor is for high heads and low flow rates. The SQFlex system has a wide voltage range, built-in maximum power point tracking (MPPT) as well as dry-running, voltage and overload protection. The specification of the solar powered submersible pump form the manufacturer used for this analysis are as the table 3.2 below:

Table 3. 2: Solar powered Submersible Pump Specification

SQF 2,5-2 N pump specification description	
Product name	SQF 2,5-2 N
Pumped liquid	Water
Maximum liquid temperature	40 °C
Liquid temperature during operation	20 °C
Density	998.2 kg/m³
Stages:	2
Maximum ambient pressure	15 bar
Pump outlet	Rp 1 1/4
Minimum borehole diameter	76 mm
Motor type	MSF3N
Power input - P1	1.4 Kw
Rated voltage ac	1 x 90-240 V
Rated voltage dc	30-300 V
Rated current	8.4 A
Power factor	1.0
Rated speed	500-3600 rpm
Start. method	direct-on-line
Enclosure class (IEC 34-5)	IP68
Insulation class (IEC 85)	F Motor
protec	Y Thermal
Udc	300 V ~ 30 V

3.9. Solar Module for the System

Photovoltaic modules constitutes the photovoltaic array of a PV system that absorb the sunlight as a source of energy to generate and supply electricity to the pump motor in our water pumping system. Several theoretical and experimental studies are made about PV water pumping systems, which are installed in many remote regions around the world to supply water for drinking and irrigation [19]. The PV array consists of an array of solar cell modules connected in series–parallel combinations to provide the desired DC voltage and current to the system. For SQF pump briefly discussed in section

3.6 of this chapter, the motor nominal power input are 1400 watt, thus a 1800 watt maximum power output from the PV panel is required to run the pumping system efficiently.

The study made by M. Benghanem, K.O. Daffallah, A.A. Joraid, S.N. Alamri, A. Jaber [19], shows for 1800 W PV generator, with PV array configurations (6S _ 4P) and (8S _ 3P) are suitable to provide the optimum energy.

For this thesis Siemens PowerMax® solar cells, solar module SP75, with 75 watt power rating each, which deliver maximum energy throughout the day, are selected with best configuration. In our case, the proposed solar panels are 24 panels module, where each generates 75 watt, connected with a best and more efficient configuration of (6S – 4P), are selected as per the analysis made for 1800watt power output arrangement of the best PV array configurations [19] which is suitable to provide the optimum energy.

The proposed PV Module are tested using manufacturer data sheets. I-V curves, P-V curves, R-V curves and I-P curves shows characteristic simulations for the Siemens PowerMax (*Appendix – B*) solar modules using the information provided by the manufacturer SIEMENS, for the products *Solar module SP75* as table 3.3.

Table 3. 3: SP75 Solar Module Specification

Solar module SP75	
Electrical parameters	12 V/6 V
Maximum power rating Pmax [Wp]	75
Rated current IMPP [A]	4.4/8.8
Rated voltage VMPP [V]	17.0/8.5
Short circuit current ISC [A]	4.8/9.6
Open circuit voltage VOC [V]	21.7/10.9
Thermal parameters	
NOCT [°C]	45 +2
Temp. coefficient: short-circuit current	2.06 mA / °C
Temp. coefficient: open-circuit voltage	- 0.077 V / °C
Qualification test parameters	
Temperature cycling range [°C]	-40 to +85
Humidity freeze, Damp heat [%RH]	85
Maximum system voltage [V]	600 V per UL (1000 V per ISPRA)
Wind Loading PSF [N/m2]	50 [2400]
Maximum distortion [°]	1.2
Hailstone impact Inches [mm]	1.0 [25]
MPH [m/s]	52 [v=23]
Weight Pounds [kg]	16.7 [7.6]

CHAPTER FOUR

4. PV DEVICE CHARACTERISTICS MODELING

First understanding the electrical characteristics of the PV module is important, since it affects the power input to PVPWP system. The output flow rate is highly depends on the power output or characteristics of the PV module. The performance of the solar powered water pumping system is evaluate by water discharge/capacity (Q) from the system, total head (TDH) of the system and electrical characteristic of the PV panel (electrical input (P) to the pump motor).

The electrical characteristics of the PV panel varies due to the variation of solar radiation throughout the day and seasonal variations. The flow rate we get from the submersible pump will vary as per the performance variation of the PV panel. Understanding this will help to model the suitable PVPWPS in a real weather condition of Jigjiga.

4.1. Ideal PV Cell

PV system directly converts sunlight into electricity. The basic device of a PV system is the PV cell. Cells may be grouped to form panels or arrays. A photovoltaic cell is basically a semiconductor diode whose *p–n* junction is exposed to light. Photovoltaic cells are made of several types of semiconductors using different manufacturing processes. PV devices present a nonlinear *I–V* characteristic with several parameters that need to be adjusted [36].

The voltage of a solar cell does not depend strongly on the solar irradiance but depends primarily on the cell temperature. PV modules can be designed to operate at different voltages by connecting solar cells in series. When solar cells absorb sunlight, free electrons and holes are created at positive/negative junctions. If the positive and negative junctions of solar cell are connected to DC electrical equipment, current is delivered to operate the electrical equipment [37]. A simplified or ideal equivalent circuit model is shown in the Figure below.

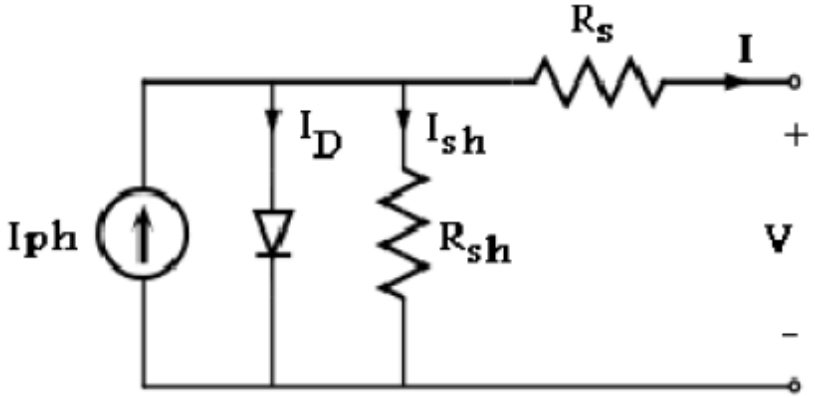

Figure 4. 1 - PV Cell Equivalent Circuit

The PV cell output voltage is a function of the photocurrent that mainly determined by load current depending on the solar irradiation level during the operation. The symbols represent; I_{ph} - Phase current , I_D - Diode current, V- Output Voltage, I_{sh} - Shunt current, R_{sh} - Shunt resister and R_s - Series resister

Figure 4.1 shows the equivalent circuit of the ideal PV cell. The basic equation from the theory of semiconductors [36], that mathematically describes the I–V characteristic of the ideal PV cell as follows;

$$I = I_{pv,cell} - I_d \tag{4.1}$$

$$I_d = I_{0,cell}\left[exp\left(\frac{qV}{akT}\right) - 1\right] \tag{4.2}$$

Where

- $I_{pv,cell}$ - current generated by the incident light (it is directly proportional to the Sun irradiation),
- I_d - Shockley diode equation,
- $I_{0,cell}$ - reverse saturation or leakage current of the diode,
- q - electron charge ($1.60217646x10^{-19}$ C),
- k - Boltzmann constant ($1.3806503x10^{-23}$ J/K),
- T (in Kelvin) - temperature of the p–n junction, and
- a - diode ideality constant.

4.2. Modeling the PV Module

PV panel Manufacturers provide basic electrical parameters about their product. Which are: the voltage at the Maximum power point (V_{mpp}), the nominal open-circuit voltage ($V_{oc,n}$), the nominal short-circuit current ($I_{sc,n}$), the current at Maximum power point (I_{mpp}), temperature coefficient for the short circuit current (K_I), temperature coefficient for the open-circuit voltage (K_V), and the maximum power output ($P_{max,e)}$. Those parameters are measured with reference to standard test conditions (STCs) of solar irradiation and cell temperature. The basic electrical parameters are not enough to investigate the performance of a PV panel. Hence, it is crucial to find out detail electrical characteristics which model the performance of PV panel.

The basic equation (4.1) of the elementary PV cell does not represent the I–V characteristic of a practical PV array. Practical arrays are composed of several connected PV cells and the observation of the characteristics at the terminals of the PV array requires the inclusion of additional parameters to the basic equation as shown in the following equation [36].

$$I = I_{PV} - I_0 \left[exp\left(\frac{V+R_S I}{V_t a}\right) - 1 \right] - \frac{V+R_S I}{R_p} \quad (4.3)$$

Where:

I_{pv} and I_0 - Photovoltaic (PV) and saturation currents of the array,

R_s - Equivalent series resistance of the array,

R_p - Equivalent parallel resistance,

$V_t = N_s kT/q$ - Thermal voltage of the array with N_s cells connected in series. Cells connected in parallel increase the current and cells connected in series provide greater output voltages. If the array is composed of N_p parallel connections of cells the PV and saturation currents may be expressed as $I_{pv,cell} = I_{pv,cell} N_p$, $I_0 = I_{0,cell} N_p$

Equation (4.3) describes the single-diode model presented in Figure 4.2. Some authors have proposed more sophisticated models that present better accuracy and serve for different purposes [36].

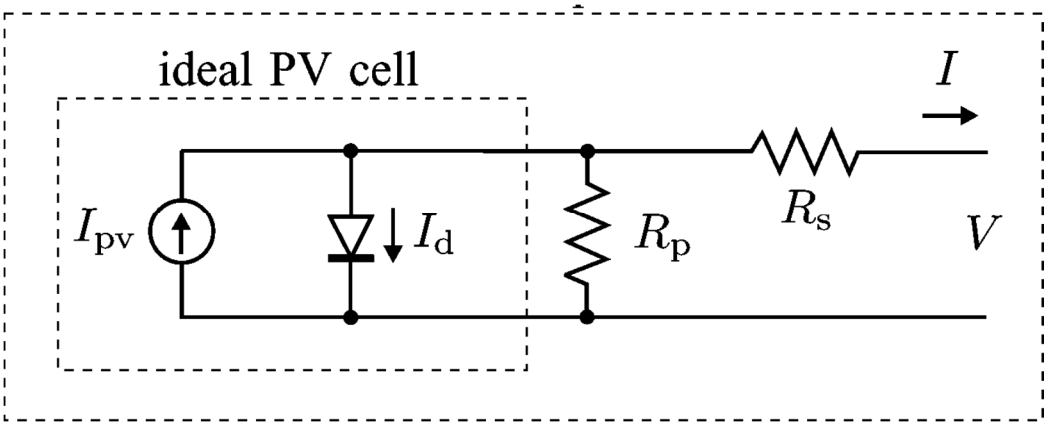

Figure 4. 2 - Single-diode Model of the Theoretical PV Cell and Equivalent Circuit of a Practical PV Device Including the Series and Parallel Resistances

The diode saturation current I_0 and its mathematical relation cell temperature is expressed as [38]

$$I_0 = I_{0,n} \left(\frac{T_n}{T}\right)^3 exp\left[\frac{qE_g}{a\text{K}}\left(\frac{1}{T_n} - \frac{1}{T}\right)\right] \quad (4.4)$$

Where E_g is the band gap energy of the semiconductor (E_g= 1.12 eV for the polycrystalline Si at 25 ˚C) and $I_{0,n}$ is the nominal saturation current, the value of diode ideality constant is ranges between 1≤ a ≤1.5 and for silicon-poly material is around 1.3.

Meanwhile the nominal diode saturation (reverse) current is given as follows [39]:

$$I_{0,n} = \frac{I_{sc,n}}{exp(V_{oc,n}/aV_{t,n}) - 1} \quad (4.5)$$

With $V_{t,,n}$ being the thermal voltage of N_s series-connected cells at the nominal temperature T_n. The insolation and temperature dependency of light-generated current of the PV cell is given by [40]:

$$I_{\text{pv}}(G,T) = \left(I_{Pv,n} + \text{Ƙ}_I \Delta T\right)\frac{G}{G_n} \tag{4.6}$$

Where $I_{Pv,n}$ (in amperes) is the light-generated current at the nominal condition (usually 25 ˚C and 1000 W/m^2), ΔT $= T - T_n$ (T and T_n being the actual and nominal temperatures [in Kelvin], respectively), G (watts per square meters) is the irradiation on the device surface, and G_n is the nominal irradiation.

The nominal light generated current $I_{Pv,n}$ can be expressed with accurate equation of the following [36].

$$I_{Pv,n} = \frac{R_P + R_S}{R_P} I_{sc,n} \tag{4.7}$$

So, equation (4.3) can be formulated with the known electrical parameters given by the manufacturer's data sheet (which are $I_{sc,n}$ and $V_{oc,n}$), the constants (a, q, E_g, Ƙ), and the external influential factors of radiation intensity and cell temperature (T, G), but the internal influencing parameters (R_s and R_P) are still unknown.

Marcelo G. et al. [36], proposed an interesting method in which the internal parameters R_s and R_P are iterated (with mathematical equation which relates the two) until the resulting pair of value $\{R_s, R_P\}$ ensures the maximum power calculated by the I–V model ($P_{max,m} = I_{mpp} \times V_{mpp}$) of equation (4.8) equal to the maximum experimental power ($P_{max,e}$) of the data sheet at the MPP (where MPP is a maximum power point, which means a point where the power output of the solar panel will be maximum).

The calculated maximum current output of the solar panel at nominal temperature and solar radiation (at 25 ºC and 1000 W/m^2) could be expressed using equation (3) as:

$$I_{mpp} = I_{\text{pv,n}} - I_{0,n}\left[exp\left(\frac{V_{mpp} + R_s I_{mpp}}{V_{t,n} a}\right) - 1\right] - \frac{V_{mpp} + R_s I_{mpp}}{R_P} \tag{4.8}$$

Where V_{mpp} is voltage at MPP (maximum power point), the thermal voltage of the panel at STC

I_{mpp} is current at MPP.

Equation (4.8) is arranged in such a manner to express the shunt resistor with other variables as follows:

$$R_P = \frac{V_{mpp} + R_s I_{mpp}}{I_{\text{pv,n}} - I_{0,n}\left[exp\left(\frac{V_{mpp} + R_s I_{mpp}}{V_{t,n} a}\right) - 1\right] - I_{mpp}} \tag{4.9}$$

From equation (4.9) R_P is expressed not only in terms parameters such as $I_{pv,n}$,$I_{0,n}$, and $V_{t,n}$, but also the nominal maximum power point (i.e. I_{mpp} and V_{mpp}) and the R_S, hence the resulting graph due to the pair values (i.e. R_S and R_P) will surely pass through the nominal maximum power points.

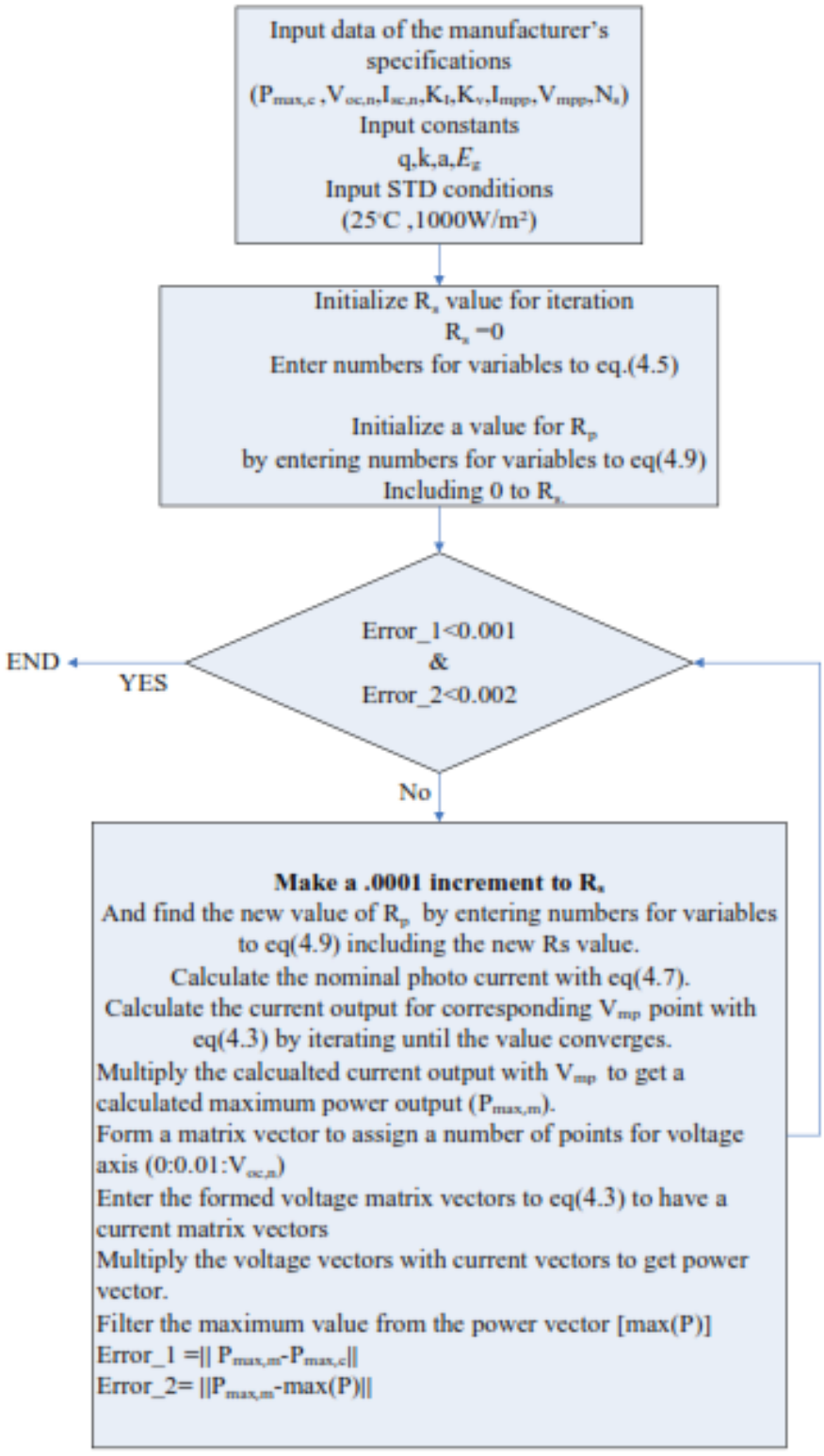

Figure 4. 3 - Algorithm of the matlab program used to model a PV panel

4.3. Operating Temperature and Efficiency of PV Module

According to the equations in section 4.2; solar irradiance intensity (G) and cell operating temperature (T) are the two crucial parameters which nonlinearly affect the current–voltage as well as power-voltage characteristics of a PV module [41]. In order to model the electrical characteristics of the PV module and its power output, first it is required to determining the cell operating temperature (T) of the PV module.

Standard heat transfer mechanics must be considered to calculate the appropriate energy balance on the cell array which leads to the estimation of operating cell temperature. At steady-state conditions, only convection and radiation heat transfers are often considered, since they are dominant over the conduction heat transfer which merely transports heat toward the surfaces of the mounting frame (especially in the case of rack-mounting free-standing arrays) [42].

A number of empirical formulas exist in various literatures whose significance appears to be best and simplest. Hence, it has been chosen an equation which is explicit, depend on easily measurable parameter and, have wide applicability. For variations in ambient temperature and irradiance, the cell operating temperature (T) can be estimated quite accurately in ^{o}C with the linear approximation [43].

$$T = T_a + \frac{G}{G_{NOCT}} \left(T_{NOCT} - T_{a,NOCT}\right) \tag{4.10}$$

Where T is the cell operating temperature of the PV module which determines the performance of the PV panel along with solar radiation intensity G, T_{NOCT} is nominal operating cell temperature which is a reference temperature for particular PV module to calculate cell operating temperature (T) and it is given by the manufacturer's specification. The nominal cell temperature (T_{NOCT}) is defined as the temperature of the cell at the conditions of the nominal terrestrial environment (NTE) [43]: Solar irradiance G_{NOCT}= 800 W/m^2, ambient temperature $T_{a,NOCT}$ = 20 ^{o}C, and average wind speed 1 m/s. Hence equation (4.10) can be expressed as follows.

$$T = T_a + \frac{G}{800\ W/m^2} \left(T_{NOCT} - 20\,^{o}C\right) \tag{4.11}$$

4.4. Optimum Tilt Angle of the Solar Panel

Facing a collector toward the equator (for our case, Jigjiga is at the Northern Hemisphere, this means facing it south) and tilting it up at an angle equal to the local latitude is a good rule-of-thumb for annual performance [44].

To prove the claim first considering the apparent sun path on the sky. The solar radiation reaches pick at solar noon when the sun just becomes at meridian of the point. So, to utilize this pick solar radiation, our solar panel must face south with zero azimuth angle (i.e. no tilting of the panel towards west or east).

For south facing panels incident angle of solar rays is given as the next equation [45]:

$$\cos(\theta) = \sin(L - \beta)\sin(\delta) - \cos(L - \beta)\,cos(\delta)cos(H) \qquad (4.12)$$

Where: θ is incident angle of solar radiation on the PV panel which is tilted by β angle from horizontal surface to south, L is latitude angle of the point, H is hour angle, and δ is declination angle.

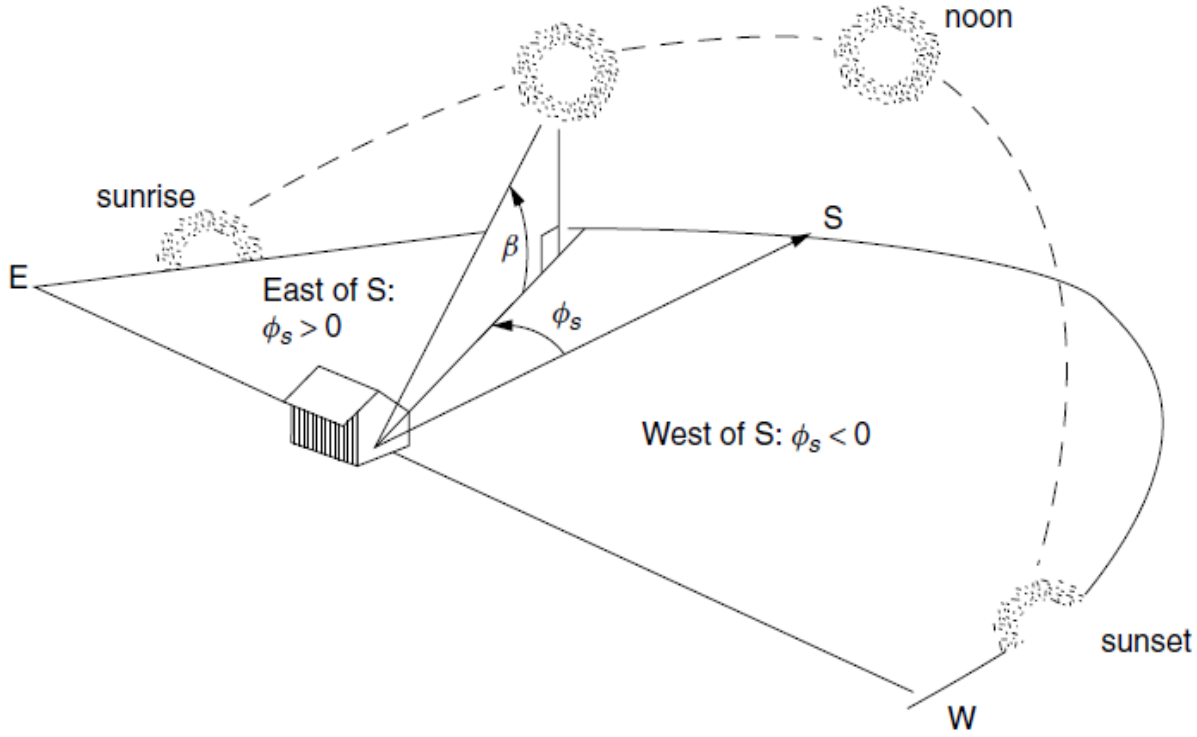

Figure 4. 4 - Apparent Solar Path on the Sky[44]

At solar noon (as it is important reference for almost all solar calculation [45]) the hour angle (H) will be zero. So, equation (4.12) will be analyzed as follows:

$$\cos(\theta) = \sin(L - \beta)\sin(\delta) - \cos(L - \beta)\,cos(\delta)cos(0)$$
$$\cos(\theta) = \sin(L - \beta)\sin(\delta) - \cos(L - \beta)\,cos(\delta)$$

Which can be further reduced using cosine law

$$\cos(\theta) = -\cos(L - \beta + \delta) \qquad (4.13)$$

$$\theta = \pi - (L - \beta + \delta) \quad (4.14)$$

Taking summer solstice or fall equinox as reference, the declination angle δ will be fixed to zero, and equation (4.14) become.

$$\theta = \pi - (L - \beta) \quad (4.15)$$

The incident angle (θ) of equation (4.15) will become optimum when its value is zero. So, does the tilt angle of the panel.

$$0 = \pi - (L - \beta_{optimum})$$

$$\beta_{optimum} = L - \pi \quad (4.16)$$

Equation (4.16) indicates the need for tilting of the solar panel at the same latitude angle but to opposite direction (i.e. if the latitude position is north to face the panel to south).

In our case, Jigjiga is found 9.38° of north. Hence the solar panel should face *9.38° to south***.** Putting equation (4.16) into equation (4.14).

$$\theta = \delta + 2\pi = \delta \quad (4.17)$$

Equation (4.17) shows that adjusting the tilt angle of the solar panel to its optimum position, will result the incident angle (θ) of solar radiation to be equal to declination angle (δ) only at solar noon time. We know that declination angel varies from -23.45° to 23.45° throughout the year, hence we can conclude that incident angle of solar radiation on optimally tilted panel varies from -23.45° to 23.45° throughout the year only at noon time [45].

4.5. Incidence Angle, θ of the Optimally Tilted PV Panel

It has been derived that the incident angle (θ) of the optimally tilted PV panel is equal to the declination angle (δ), but this happens only at noon time where the hour angle (H) is zero. So, we have to visualize the variation of the incident angles at other hour angles.

Putting equation (4.16) to equation (4.12) we got an equation to express for incident angle and derived as follows.

$$\cos(\theta) = \sin(\pi)\sin(\delta) - \cos(\pi)\cos(\delta)\cos(H)$$

$$\cos(\theta) = -\cos(\pi)\cos(\delta)\cos(H)$$

$$\cos(\theta) = \cos(\delta)\cos(H) \quad (4.18)$$

Where the declination angle, δ in degrees for any day of the year (N) can be calculated approximately by the ASHARAE equation [45]:

$$\delta = 23.45 \sin\left[\frac{360}{365}(284 + N)\right] \quad (4.19)$$

Table 4. 1: Day Number for Each Month

Month	***Day Number***
January	i
February	31+i
March	59+i
April	90+i
May	120+i
June	151+i
July	181+i
August	212+i
September	243+i
October	273+i
November	304+i
December	334 +i

The hour angle can also be obtained from the Apparent Solar Time (AST); that is, the corrected local solar time [45]:

$$H = (AST - 12)15 \tag{4.20}$$

At local solar noon, apparent solar time, AST=12 and hour angle, H = 0^o. Therefore, the LST (the time shown by our clocks at local solar noon) is:

$$LSN = 12 - ET + 4(SL - LL) \tag{4.21}$$

Where LSN is local solar noon which is shown by our clock, SL is standard longitude of the country; LL is local longitude of the region (Jigjiga), ET is equation of time whose value can be obtained as a function of the day of the year (N) approximately from the following equations [45]:

$$\mathrm{ET} = 9.87\sin(2B) - 7.53\cos(B) - 1.5\sin(B)\ [min] \tag{4.22}$$

and

$$B = (N - 81)\frac{360}{364} \tag{4.23}$$

Ethiopia has standard latitude and longitude of 8^o00 north and 45^o00 east respectively, while Jigjiga has 9.35^oN latitude and 42.8^oE longitude.

Incident angle (θ) for a horizontal surface is equal to zenith angle (Φ)

$$\theta = \Phi$$

$$\cos(\Phi) = \sin(L)\sin(\delta) + \cos(L)\cos(\delta)\cos(H) \tag{4.24}$$

4.6. Driving Beam and Diffuse Radiation Components from the Measured Global Radiation

In order to determine total radiation on the tilted surface, the global radiation data from metrological agency must be split into its Beam and diffuse component (since the measured data is a global radiation measurement on horizontal surface, it does not contain reflected radiation).

Diffuse Radiation Component

The model developed by Threlkeld and Jordan (1958), which is used in the ASHRAE Clear-Day Solar Flux Model, suggests that diffuse radiation on a horizontal surface G_{DH} is proportional to the direct beam radiation G_B no matter where in the sky the sun happens to be [44]:

$$G_{DH} = CG_B \tag{4.25}$$

Where C is a sky diffuse factor and its convenient approximation for any day of the year (N) is expressed as follows [44]:

$$C = 0.095 + 0.04 \sin\left[\frac{360}{365}(N - 100)\right] \tag{4.26}$$

The beam radiation normal to horizontal surface G_{BH} is expressed as:

$$G_{BH} = G_B \cos(\Phi) \tag{4.27}$$

Where G_B is beam radiation, and G_{BH} is beam radiation normal to a horizontal surface, and Φ is zenith angle (or incident angle on horizontal surface).

By recalling equation (4.24), zenith angle is expressed as:

$$\cos(\Phi) = \sin(L)\sin(\delta) + \cos(L)\cos(\delta)\cos(H)$$

Putting equation (4.25) to equation (4.27)

$$G_{BH} = \frac{G_{DH}\cos\Phi}{C} \tag{4.28}$$

Global radiation on horizontal surface (G_H) is a sum of beam radiation on horizontal surface (G_{BH}) and diffuse radiation on horizontal surface (G_{DH}).

$$G_H = G_{BH} + G_{DH} \tag{4.29}$$

Putting equation (4.29) and equation (4.28) all together we get:

$$G_H = G_{DH} + \frac{\cos(\Phi)G_{DH}}{C}$$

Diffuse Radiation will be expressed in terms of global radiation measured on horizontal surface (G_H) as:

$$G_{DH} = \frac{G_H}{1 + \cos(\Phi)/C} \tag{4.30}$$

With regard to our previous discussion it is obvious that G_H is a measured radiation data on horizontal surface which is provided by the metrology agency. So, with the help of equation (4.30) it is possible to drive the diffuse component of the measured radiation data [44].

Beam Radiation component

Once we calculated the diffuse radiation, it is possible to get the beam component of the measured data from equation (4.18).

Rearranging equation (4.29) we get an expressive equation to beam component:

$$G_{BH} = G_H - G_{DH} \tag{4.31}$$

4.7. Total Radiation on our (Optimally Tilted) Panel

To optimize solar radiation interception, the panel has been proposed to be tilted at angle equal to the latitude position of the region. However, as it has been mentioned, the provided radiation data was a global radiation measured at horizontal surface. Therefore, we need to generate solar radiation data on the tilted panel, by converting the existing radiation data (on horizontal surface) to radiation on the tilted surface.

Beam radiation, G_{Bt}on tilted surface is [45]:

$$G_{Bt} = G_B cos(\theta) \tag{4.32}$$

And on horizontal surface is:

$$G_{BH} = G_B \cos(\Phi) \tag{4.33}$$

Where G_B is beam radiation, G_{Bt} is beam radiation on the tilted panel, G_{BH} is beam radiation measured on horizontal surface, and θ is the incident angle, and Φ is azimuth angle.

It follows that,

$$R_B = \frac{G_{Bt}}{G_{BH}} = \frac{\cos(\theta)}{\cos(\Phi)} \tag{4.34}$$

Where R_B is called beam radiation tilt factor. In our case the term $\cos(\theta)$ can be calculated with equation (4.18), $\cos(\Phi)$ from equation (4.27), and G_{BH} has been derived from the measured data with equation (4.20). So the beam radiation component for our panel is:

$$G_{Bt} = G_{BH} R_B \quad (4.35)$$

Diffuse radiation, G_{Dt} on tilted surface is expressed in terms of diffuse radiation on horizontal surface as [45]:

$$G_{Dt} = G_{DH} \frac{1 + \cos(\beta)}{2} \quad (4.36)$$

Where β is tilt angle of the panel, and G_{DH} is the diffuse radiation which is derived with equation (4.30) from the provided global radiation data.

Reflected radiation can be modeled as the total of horizontal radiation (G_H) times the ground reflectance ρ. The fraction of the ground reflected radiation that will be intercepted by the tilted panel, G_{Rt} depends on the slope of the tilt angle of the panel β, resulting in the following expression for reflected radiation on tilt surface [45]:

$$G_{Rt} = \rho G_H \frac{1 - \cos(\beta)}{2} \quad (4.37)$$

Estimates of ground reflectance range from about 0.8 for fresh snow to about 0.1 for a bituminous-and-gravel roof, with a typical default value for ordinary ground or grass taken to be about 0.2.

The total (Global) radiation, G_t on the tilted panel is therefore

$$G_t = G_{Bt} + G_{Rt} + G_{Dt} \quad (4.38)$$

4.8. Curve and Surface Fitting for pump characteristic equation modeling

This chapter briefly discuss about curve and surface fitting to process the data analysis for the submersible pump only. This requires because the data from pump manufacturer are the curves and the resulting power P(kw), flow rate Q(m^3/hr) and head H(m) values. This values has to be first changed to the characteristic equation using this three variables to make it easy for the analysis purpose.

Pump manufacturer provide a data that only shows the resulting values and performance curves for head vs discharge, power vs discharge, efficiency vs discharge, etc. For this thesis performance simulation analysis of the PVPWP system, characteristics equation has to be generated using the available data. This can be done using Matlab to meet the objective of this research.

One can use any curve or surface fitting procedures or models to generate a characteristics equation, here we select the polynomial curve and surface fitting model because of its simplicity to summarize a relation between two or more variables.

Data processing are an ever growing number of way to dealing with such a discrete set of points [46]. The conventional approaches in curve and surface fitting aim for an approximation of the shape represented by the set of points. Generally Curve fitting or surface fitting are the process of introducing mathematical relationships between dependent and independent variables in the form of an equation for a given set of data.

Curve and surface fitting can be involve in a system either interpolation, where a particular data is required or smoothing, where smooth function is constructed that fit the data. Fitted curve or surface used to visualize data, to assume values where no data are available and to summarize the relationship between two or more variables [47].

In curve and surface fitting problems the purpose is to approximate the set of data points as closely as possible with a specified function, which is smooth as possible. The smoothness requirement is met simply by limiting the number of coefficients allowed in the fitting function [46].

The selection of a routine to treat a particular fitting problem is depend on the fitting function chosen primary. When the mathematical form of the fitting function is immaterial to the problem, polynomials and cubic splines functions are preferred because their simplicity and ease of handling a deliberate substantial benefits [46].

4.9. Polynomial Models in Curve and Surface Fitting

Polynomials have many applications in engineering and science. For instance, they are used extensively in curve-fitting [47]. The homogeneous or general solution of the equation tell us something very fundamental about the system being simulated, thus the result is a polynomial called the characteristic equation. The eigenvalue in the characteristic equation tells us something fundamental about the system we are modeling, and finding the eigenvalues involves finding the roots of polynomials [47].

The problem of least-squares curve fitting by polynomials is satisfactorily solved by a computer program based on the method described by the author *Forsythe* [48]. In this, we generate by recurrence a system of polynomials which are orthogonal with respect to summation over the particular point distribution of the problem in question.

We may then compute the coefficients' of these polynomials in a series whose truncation at any point yields the least-squares approximation of the appropriate degree. The simplest surface-fitting

problem (that is, data fitting problem in two independent variables) presents data at all the points of intersection of a rectangular mesh whose lines are parallel to the sides of a rectangular boundary.

We require a least-squares polynomial fit in the variables x and y, Cartesian co-ordinates measured along the lines of the mesh. It is easily solved by repeated application of the curve-fitting routine [47].

Generally, polynomial models for curves are given by [49]:

$$y = \sum_{i=1}^{n+1} P_i x^{n+1-i} \tag{4.39}$$

Where: $n + 1$ is the *order* of the polynomial, n is the *degree* of the polynomial, and $1 \leq n \leq 9$. The order gives the number of coefficients to be fit, and the degree gives the highest power of the predictor variable.

Polynomials are described in terms of their degree. For example, a third-degree (cubic) polynomial is given by:

$$\gamma = p_1 x^3 + p_2 x^2 + p_3 x + p_4 \tag{4.40}$$

Polynomials are often used when a simple empirical model is required. We can use the polynomial model for interpolation or extrapolation, or to characterize data using a global fit.

The main advantages of polynomial fits include reasonable flexibility for data that is not too complicated, and they are linear, which means the fitting process is simple. The main disadvantage is that high-degree fits can become unstable. Additionally, polynomials of any degree can provide a good fit within the data range, but can diverge wildly outside that range.

When we fit with high-degree polynomials, the fitting procedure uses the predictor values as the basis for a matrix with very large values, which can result in scaling problems. To handle this, normalize the data by centering it at zero mean and scaling it to unit standard deviation [49]. In computer program Matlab we can control the terms to include in the polynomial surface model by specifying the degrees for the *x* and *y* inputs.

CHAPTER FIVE

5. RESULT AND DISCUSSIONS

Here in this thesis a solar water pumping system is analyzed. Where SQF helical type solar submersible pump is selected to be the heart of system which will be coupled with a PV module of SP75. In this case, no battery is required since water to be stored.

The modelling of the system is done under the weather condition of Jigjiga, annual temperature and global radiation (i.e. Pyranometer) data from Ethiopian National Metrology Agency is provided which is measured in 15 minutes' difference for each days of the years.

5.1. Meteorological Data Analysis

Data analysis of the measured data for global radiation and temperature are discussed briefly, by analyzing the raw data measured using Pyranometer and compare this measured raw data on optimally tilted panel. The data obtained from Ethiopia National Meteorology Agency are measured using Pyranometer in every 15 minutes for the entire 24 hours duration of the day automatically for both solar radiation in (W/m^2) and temperature in (^oC).

This data obtained from the Agency are for a years of (2011-2019), for the whole 12 months each day in every 15 minutes, which tabulated in excel sheet. Using Matlab programing these solar radiation and temperature data were sorted for specific dates. Change the measured (Pyranometer) radiation data which is measured on horizontal surface into expected radiation intensity on the optimally tilted panel, compare incident angle of our tilted panel to zenith angle. (Note that, zenith angle is incident angle of horizontally positioned panel) and calculate cell temperature. This data analysis gives us all the required data to enter to the PV panels basic Equation 4.3 in section 4.2 of the chapter 4 to get electrical power output from the solar module (like voltage, current and power output).

5.2. Data Sorting for the Specified Dates

The raw data obtained from the agency are very bulky, therefore, there should be a mechanism to sort out the global radiation and temperature data for specified dates. A Matlab program is developed which is capable of sorting out this raw data for which considers the mathematical sequence by which the data is presented. This Matlab program gives global radiation and temperature of the specific dates in 24 hours format graphically as presented in the Figures below.

Choosing one day for each 12 months, the graphical data presented here shows temperature and radiation intensity throughout the day.

Klein recommended the average day for each month as can be seen in Table 6.1. thus the data presented for the representative days of the months as recommended by Klein S.A. [50].

Table 5.1. Average day for each month as recommended by Klein [50].

Month	Date	Day of the Year
January	17 January	17
February	16 February	47
March	16 March	75
April	15 April	105
May	15 May	135
June	11 June	162
July	17 July	198
August	16 August	228
September	15 September	258
October	15 October	288
November	14 November	318
December	10 December	344

Figure 5.1 to 5.3, shows hourly radiation and hourly temperature variation of a 24 hours in a day for the months of January, May, and September in the average representative days of the months recommended by klein, which is 17th January, 15th May and 15th September. This three months are selected because the major seasonal variation differences in solar radiation and temperature shown clearly in this months.

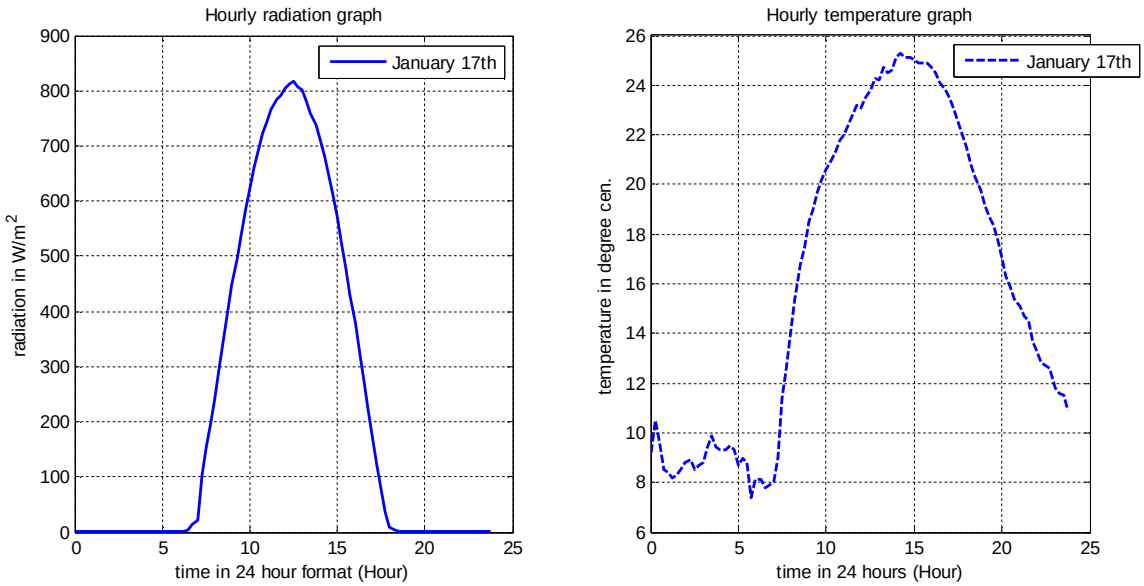

Figure 5. 1 – Global Radiation and Temperature Data for Jan. 17th

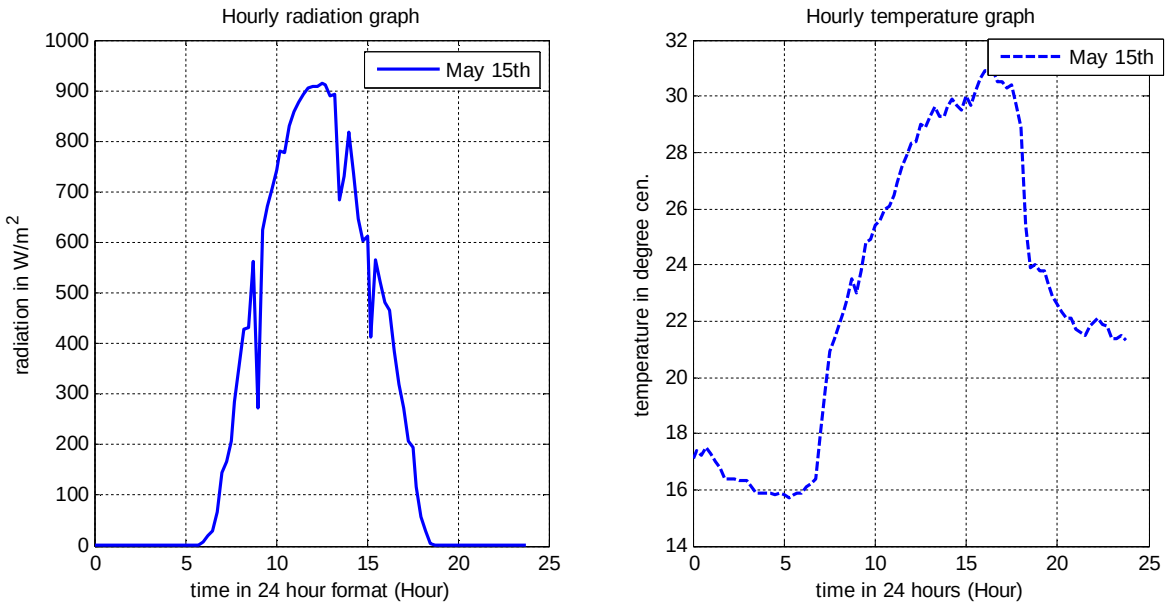

Figure 5. 2 – Global Radiation and Temperature Data for May 15th

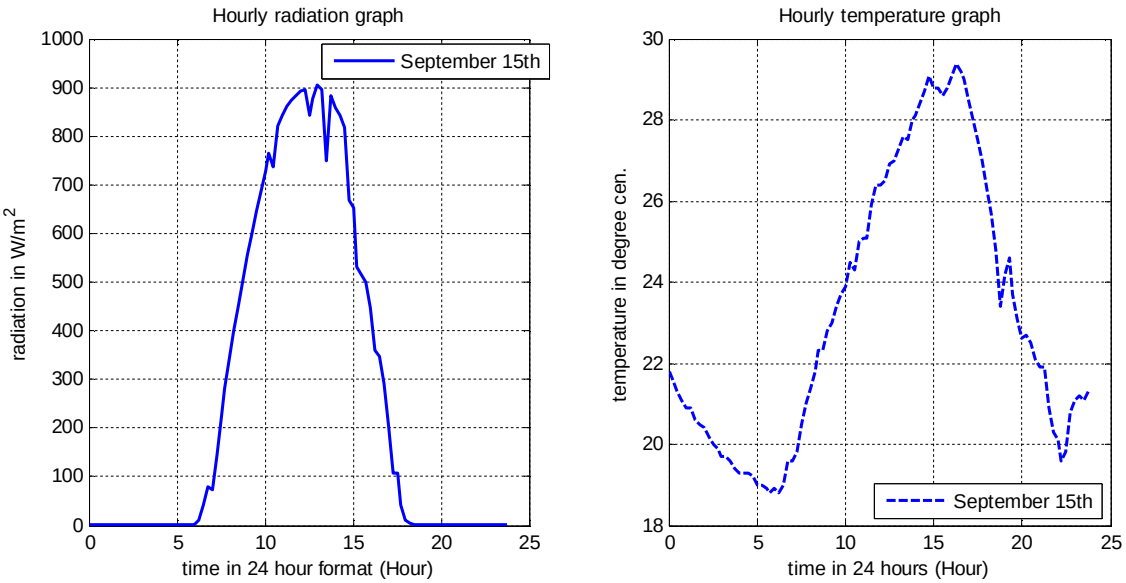

Figure 5. 3 – Global Radiation and Temperature Data for Sep. 15th

Any month and day can be selected for the hourly performance simulation system to determine the output result and model the PVPWP system, but in our case all the data sorting and simulation of the PVPWP system are done for the 17th January, 15th May and 15th September day of this three months. Data analysis result of solar radiation and temperature using the given data for JigJiga, which is the result of Matlab program codes, are as shown in the Figures above.

5.3. Compare Measured Global Radiation and Total Radiation Variation on Optimally Tilted Panel

In this section the measured global radiation and total radiation on optimally tilted panel will be compared. The generated Matlab code will change the measured (Pyranometer) radiation data which is measured on horizontal surface into expected radiation intensity on optimally tilted panel, since the panel we use are tilted as discussed in chapter 4. This code will also compare incident angle of our tilted panel to zenith angle (note that zenith angle is incident angle of horizontally positioned panel), it determines radiation flux on horizontally positioned panel, while the incident angle determines radiation flux on tilted panel. Therefore, we can judge the improvement of radiation flux due to the tilting of the panel rather than positioning it horizontally (incident angle is related to flux).

The graph shown here checked for all 12 months of the year. Hence, it identifies that, tilting a panel at its optimum angle will not give a better flux throughout a year, but it rather improved the annual PV panel performance.

Figure 5.4 to 5.6 shows the comparison of incident angle and zenith angle curves and the comparison of total radiation curves on tilted panel and horizontal plane, with 24 hours format in a day for the months of January, May, and September in the 17th January, 15th May and 15th September day of the months. Which is the result of Matlab program codes.

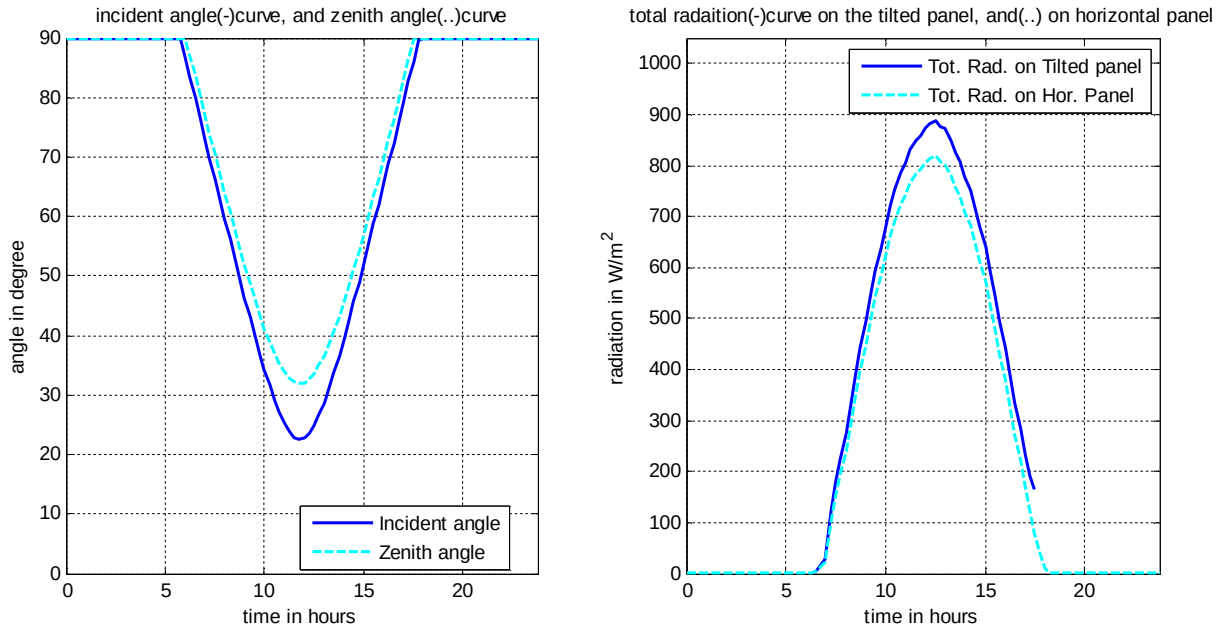

Figure 5. 4 - Incident Angle and Zenith Angle Curves, and Total Radiation on Tilted Panel and Horizontal Plane for Jan. 17th

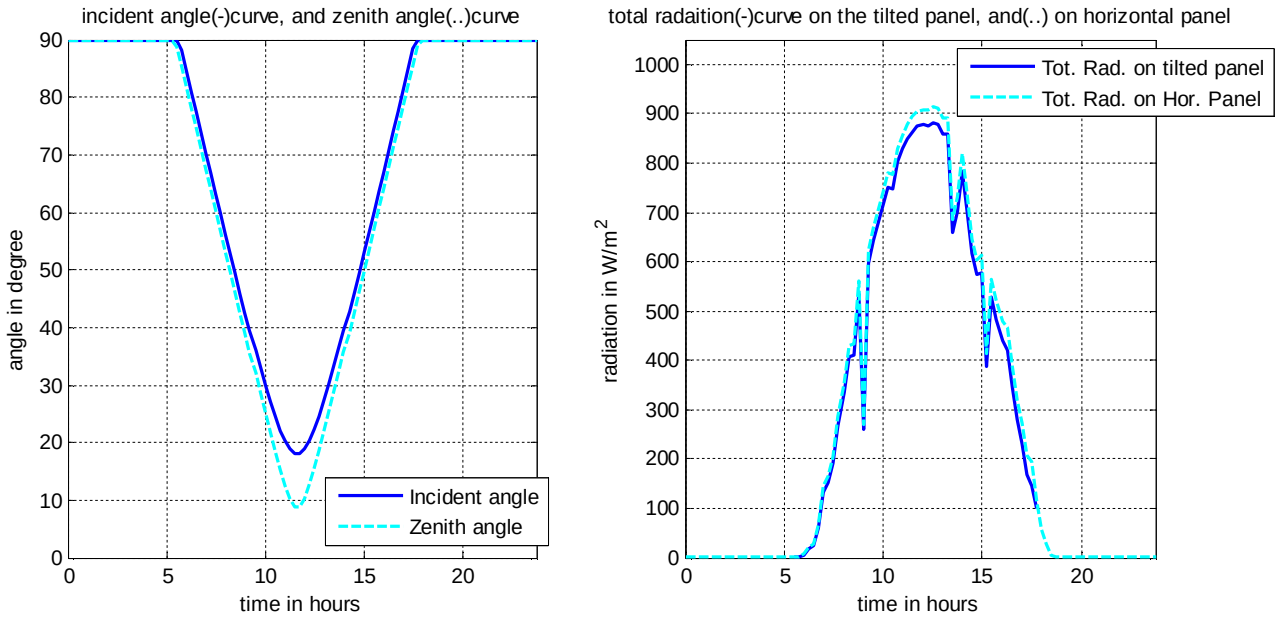

Figure 5. 5 - Incident Angle and Zenith Angle Curves and Total Radiation Curves on Tilted Panel and Horizontal Plane for May 15th

The graphs indicates, in months of September, November, December, January, February and march there are an improvement in radiation flux due to the tilting of the panel into its optimum angle. As described on the graphs, for this months the incident angles are traced below the zenith angles, the lower the incident angle is a higher in radiation flux.

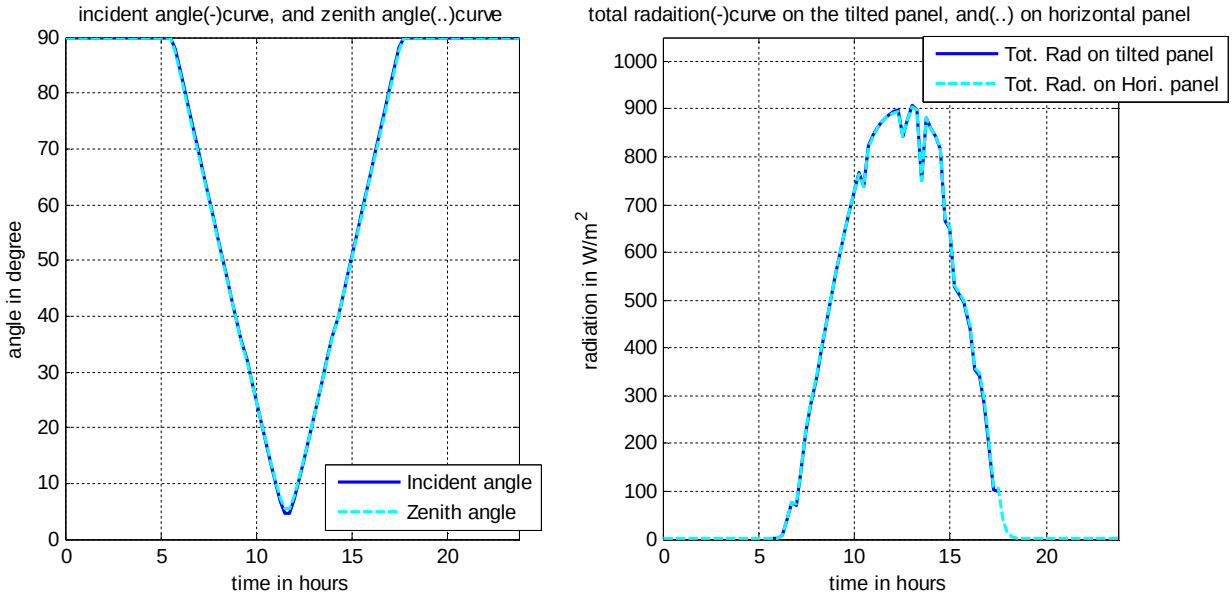

Figure 5. 6 - Incident Angle and Zenith Angle Curves and Total Radiation Curves on Tilted Panel and Horizontal Plane for Sep. 15th

For months from April to August the radiation flux on the tilted panel are not improved, rather it is lower than the horizontally positioned panel. Thus we will have a better performance on horizontally positioned panel. Hence we can conclude that, tilting a PV panel on its optimum position will results a general improvement in PV panel performance, but it will not give a better performance thought out the year.

The other option to have a better performance throughout the year is changing the panel from tilted position to horizontal surface position, in months of April, May, June, July and August to improve the radiation flux on the PV panel, manually (without using any tracking device). In this case our system can be in its optimum position and will give a better performance throughout the year.

5.4. Hourly Variation of Operating Cell Temperature of the Array

As briefly discussed in chapter 4 section 4.3, solar irradiance intensity (G) and cell operating temperature (T) are the two essential parameters, which nonlinearly affect the current–voltage as well as power-voltage characteristics of a PV module [41]. In order to model the electrical characteristics of the PV module and its power output, first it is required to determining the cell operating temperature of the PV module.

The following Figure 5.7 shows the hourly cell temperature variation graph generated in ^{o}C in 24 hours formats for the months of January, May and September representative days of 17th January, 15th May and 15th September.

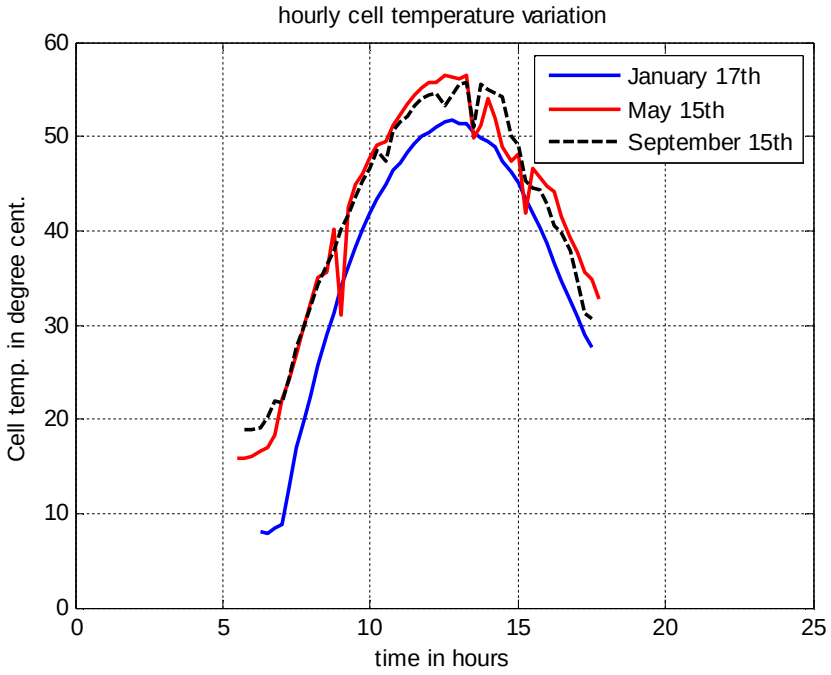

Figure 5. 7 - Hourly Cell Temperature Variation

5.5. Pump Characteristic Equation by Curve/Surface Fitting Polynomial Model

Using the manufacturer SQF helical type solar submersible pump curve and the data values of power and discharge at a given heads [51], as shown in *Appendix A- 1.1 and 1.2*, generate surface fitting equation using Matlab simulation which arrange the points in (XYZ) form, where X=Power P(kw), Z=Flowrate Q(m^3/hr) and Y=Head H(m).

The polynomial function fitting equation generated using Matlab relates flowrate as a function of head and power Q=Q(P,H). The polynomial function equation generated simulate flow rate Q using solar radiation and temperature data for the total heads of 90, 80, 70, 60 and 50 m respectively. Then comparing the output flowrate result of this modeling with the experimental analysis made in Madinah located in Saudi Arabia [18].

The polynomial characteristics equation generated using Matlab shown below are by using manufacturer curve and then surface fit by taking different points of flow rate Q, power P and head H readings and taking this points are a data feed to the Matlab linear model program for polynomial function (3,3).

Linear model Poly33:

sf(x,y) = p00 + p10*x + p01*y + p20*x^2 + p11*x*y + p02*y^2 + p30*x^3 + p21*x^2*y + p12*x*y^2 + p03*y^3

Coefficients (with 95% confidence bounds):

p00 =	1.291	(0.6246, 1.958)
p10 =	8.303	(7.809, 8.797)
p01 =	-0.05589	(-0.08582, -0.02596)
p20 =	-3.211	(-3.717, -2.705)
p11 =	-0.03889	(-0.05462, -0.02315)
p02 =	0.0005047	(5.997e-05, 0.0009494)
p30 =	-1.373	(-1.79, -0.9552)
p21 =	0.06073	(0.0497, 0.07177)
p12 =	-0.0003439	(-0.0004932, -0.0001946)
p03 =	-1.161e-06	(-3.36e-06, 1.037e-06)

The resulting fitting graph for the pump performance equation analysis from the curve and surface fitting by polynomial function using Matlab, for 50, 60, 70, 80 and 90 meter head (which are a blue dots in the graph below), where Y axis is for head (H), Y axis is for Power (P) and Z axis is for flow rate (Q), are as indicated in Figure 6.8 below. ☺

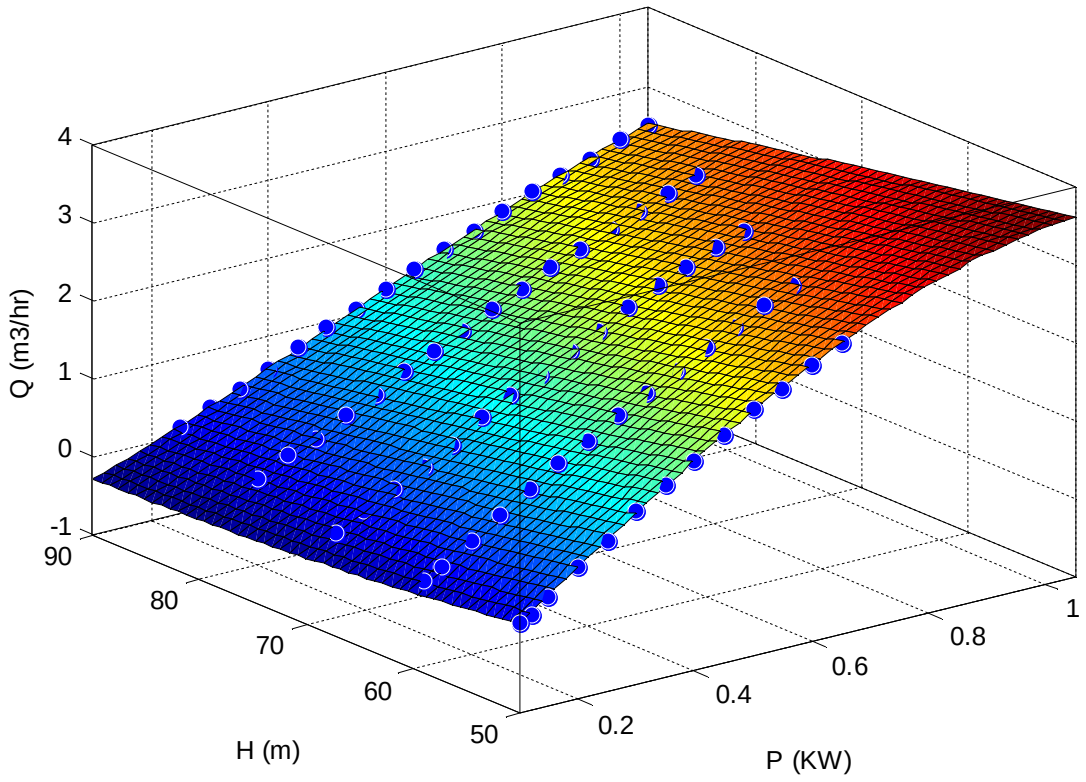

Figure 5. 8 - A Graphical Representation of the Curve and Surface Fitting Characteristic Equation

5.6. Matlab Simulation Result of SP75 PV Module and Array

As per the manufacturer specification of [52], a computer program result for the selected PV module are presented here as shown in the Figures below using Matlab programing with configuration of six series and four parallel connection (6S – 4P).

The I-V curves as shown in *Figure 5.9*, and *Figure 5.12* describe the simulation results for current versus voltage characteristics of the photovoltaic modules with the operating cell temperature of 25^{o}C and the effective irradiance level changing of, 200W/m^2, 400W/m^2, 600W/m^2, 800W/m^2, and 1000W/m^2. Where the simulated I-V curves are similar to the I-V curves provided by manufacturer [52]. Other curves such as: P-V curves, R-V curves and I-P curves, which is not provided by the manufacturer can be calculated using the proposed model programming. This curves information are very important for solar power systems where the irradiance level changes quickly throughout the day.

Similarly, the P-V, and R-V curves shown in *Figure 5.10, Figure 5.11, and Figure 5.13* are power versus voltage as well as module resistance versus current characteristics of a single module at different effective irradiation level and 25^{o}C cell temperature of the panel and solar array.

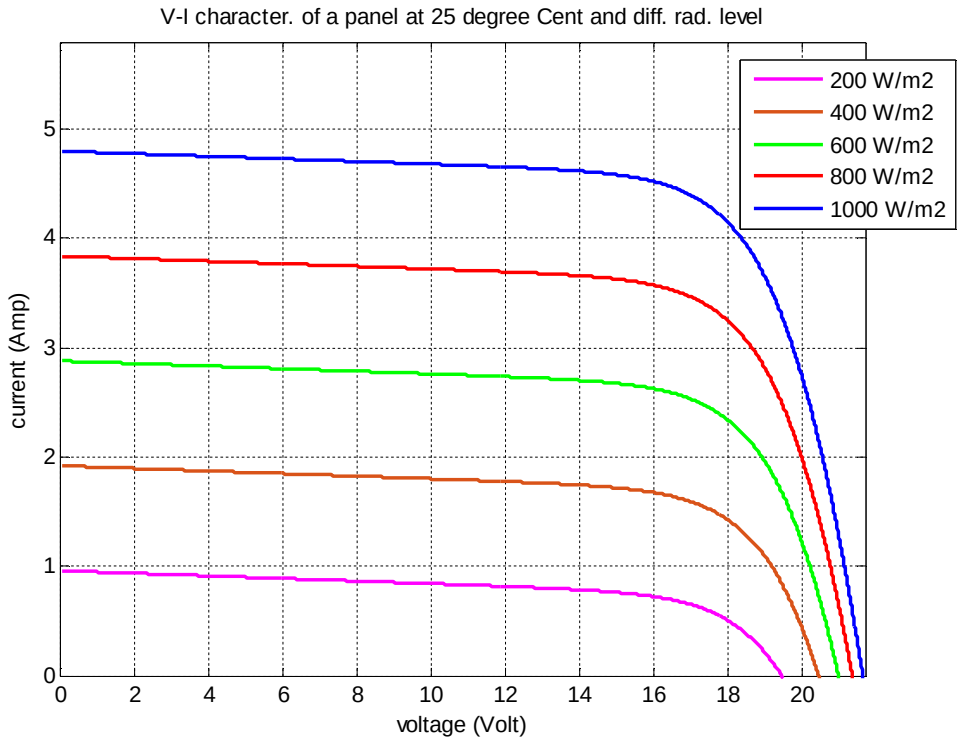

Figure 5. 9 - V-I Characteristic of a Panel at 25 ºC and Different Radiation Level

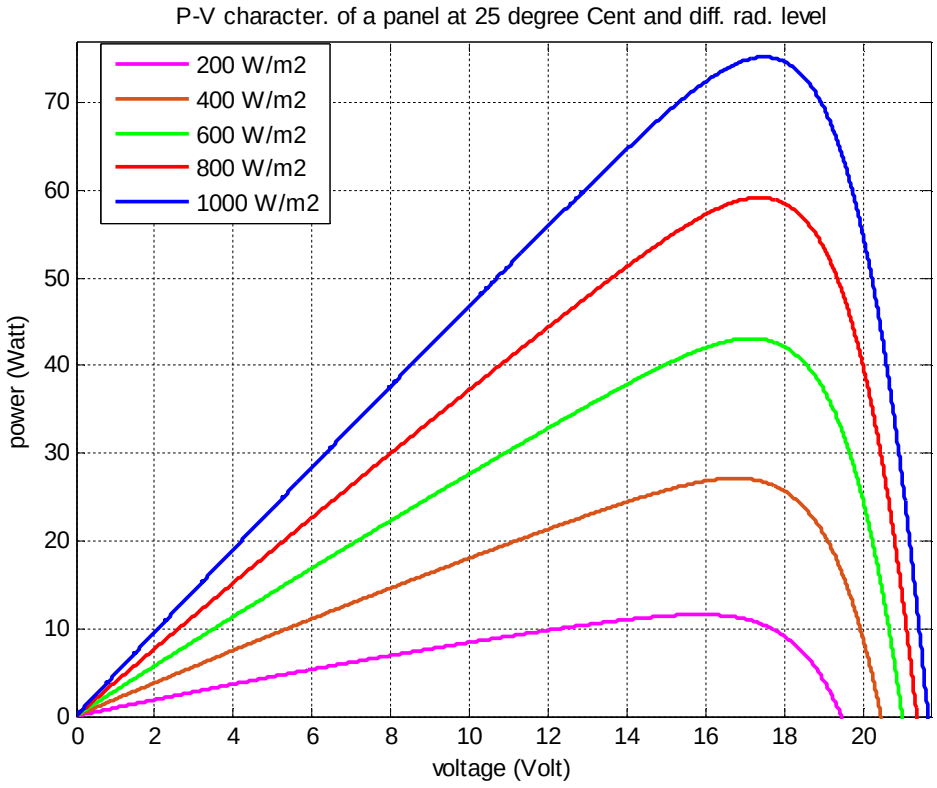

Figure 5. 10 - P-V Characteristic of a Panel at 25 ºC and Different Radiation Level

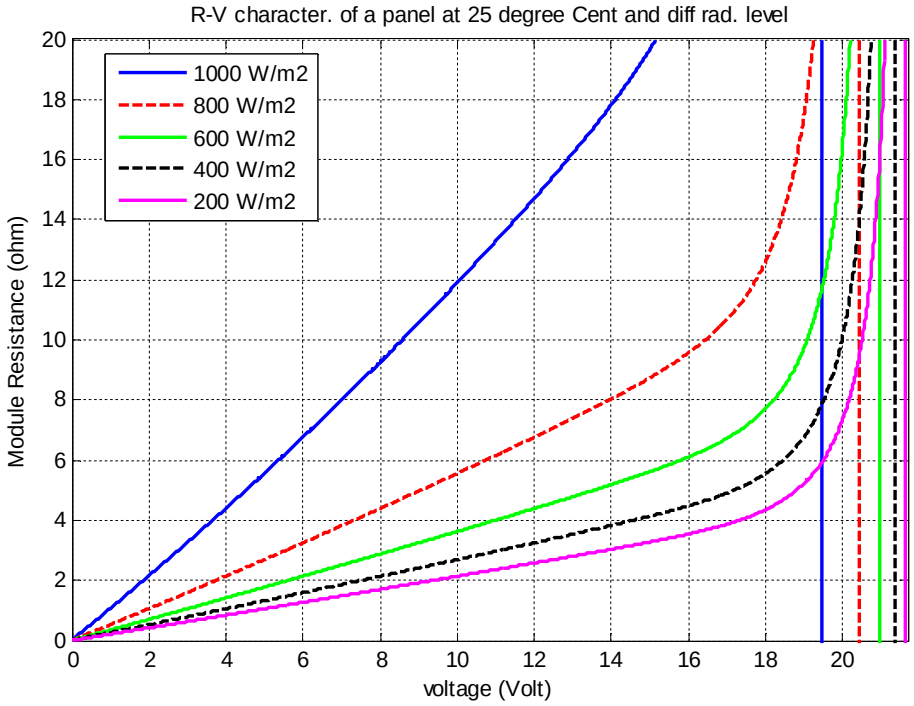

Figure 5. 11 - R-V Characteristic of a Panel at 25 ^{o}C and Different Radiation Level

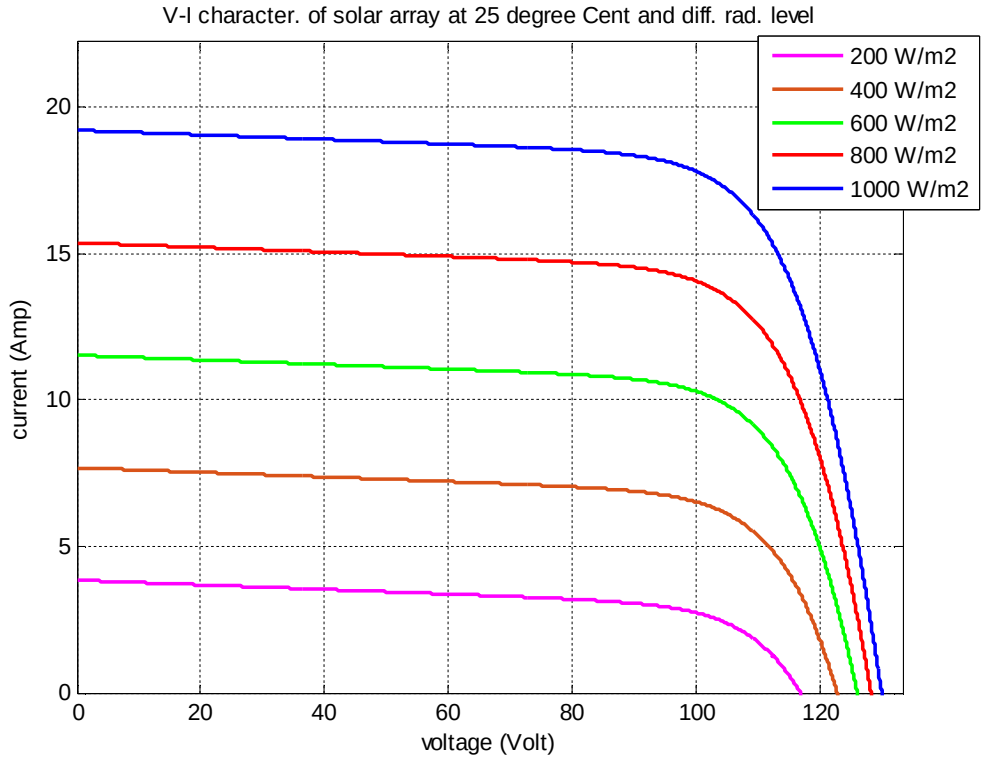

Figure 5. 12 - V-I Characteristic of a Solar Array at 25 ^{o}C and Different Radiation Level

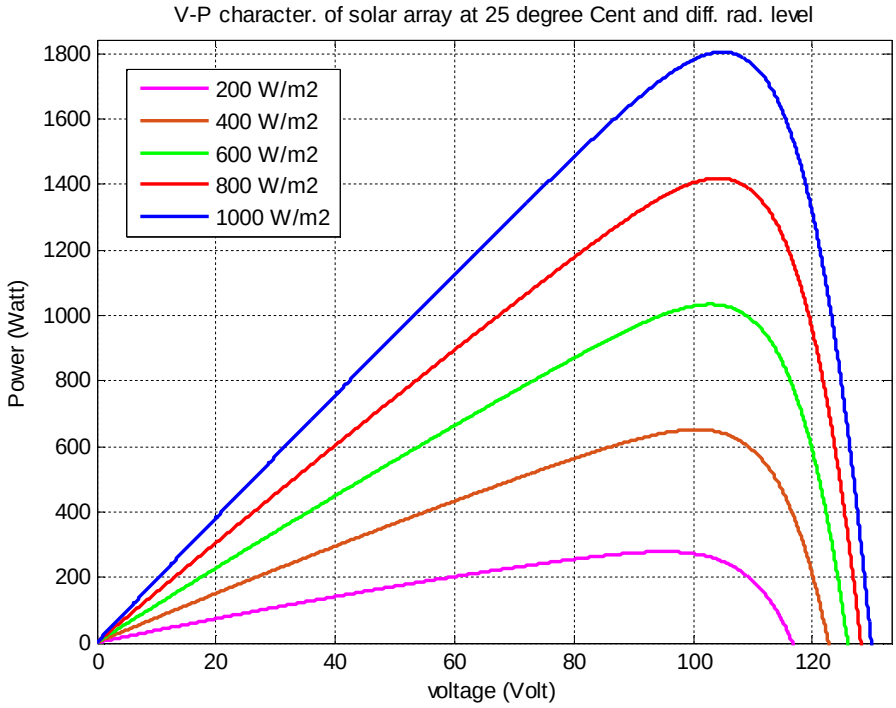

Figure 5. 13 - V-P Characteristic of a Solar Array at 25 ^{o}C and Different Radiation Level

Figure 5.14 below shows simulation results for I-V curve of the photovoltaic module SP75 under different temperatures of operation (i.e. 25^{o}C, 50^{o}C and 75^{o}C) with the irradiation level at 1000W/m^2. Figure 5.15 shows how the temperature effect on the maximum power supplied by the photovoltaic module under a constant irradiance level of 1000W/m^2 and Figure 5.16 shows resistance versus current characteristics at different operation temperatures with the irradiation level at 1000W/m^2.

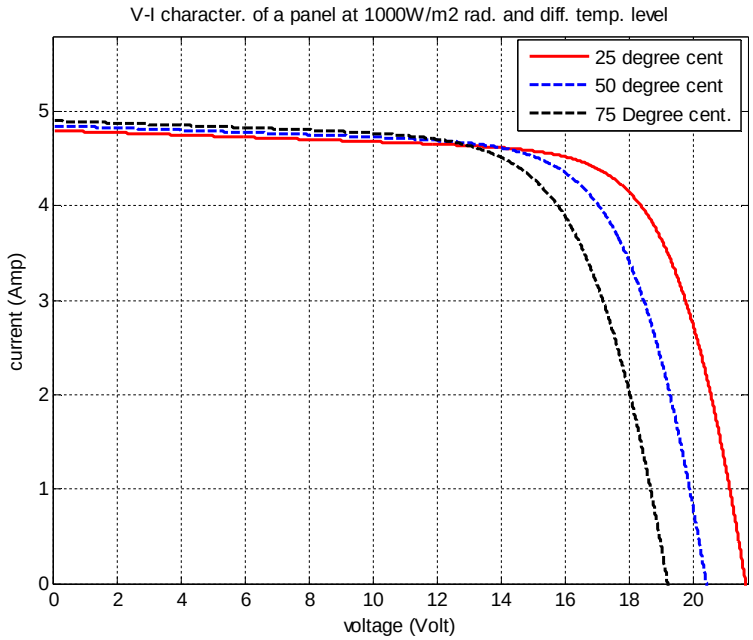

Figure 5. 14 - V-I Characteristic of a panel at 1000 W/m^2 radiation and different temperature Level

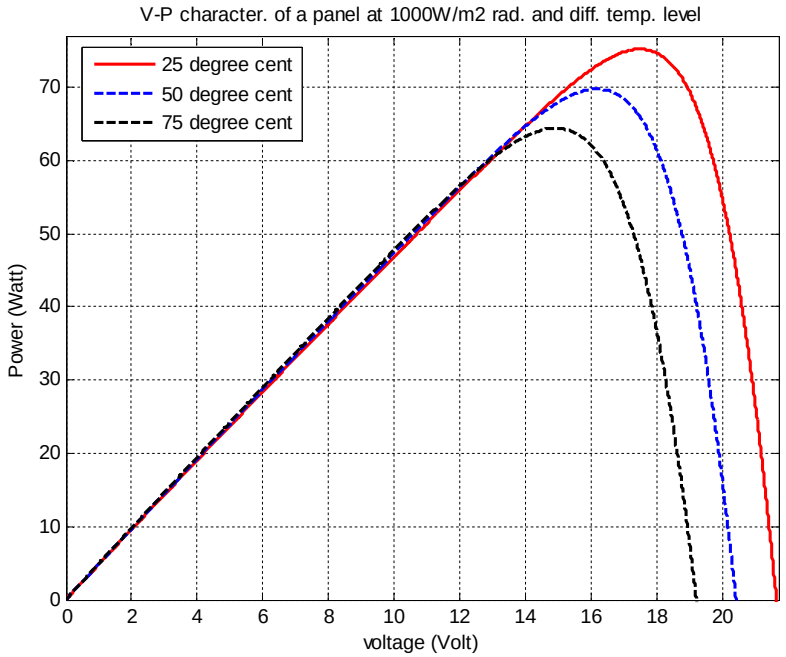

Figure 5. 15 - V-P Characteristic of a panel at 1000 W/m^2 radiation and different temperature level

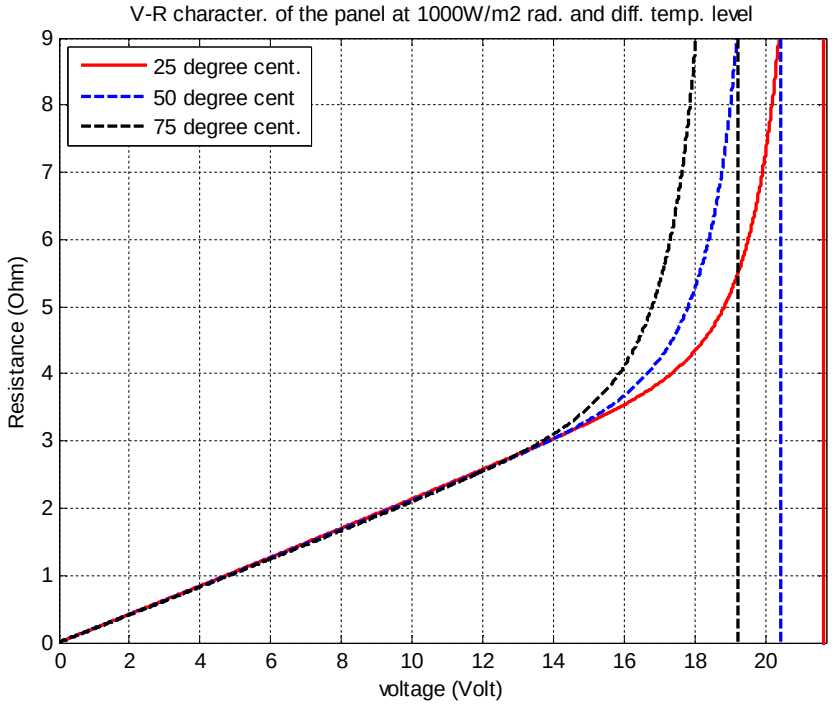

Figure 5. 16 - V-R Characteristic of a panel at 1000 W/m^2 radiation and different temperature level

5.7. Hourly Variation of Electrical Characteristic Output of the PV Array

This section is focused on hourly performance simulation of a PV panel. The electrical characteristics of the PV panel varies due to the variation of solar radiation and temperature throughout the day and through seasonal differences[53].

The following Figures shows hourly power, current, voltage and efficiency of the PV panel for the average day for each month as recommended by Klein of January, May and September. The result of hourly variation of power output of this analysis, is the input parameter to the pump polynomial function equation discussed in section 6.5 of this chapter. The PV array power output shown in Figure 5.17 in 17th January, 15th May and 15th September, in noon time the output power reaches 1500 W, which is the maximum output through a day. During morning and evening the nominal output power of the panel will be almost zero, since the solar radiation is less during this time. This is done using metrological data input and equations briefly discussed in chapter four of this research.

Figure 5.18 and Figure 5.19 show hourly current and voltage variation of the PV array throughout a day. Figure 5.20 shows efficiency variation of the PV panel throughout a day. The efficiency reaches its maximum point during maximum solar radiation time and stay almost constantly during this maximum radiation time.

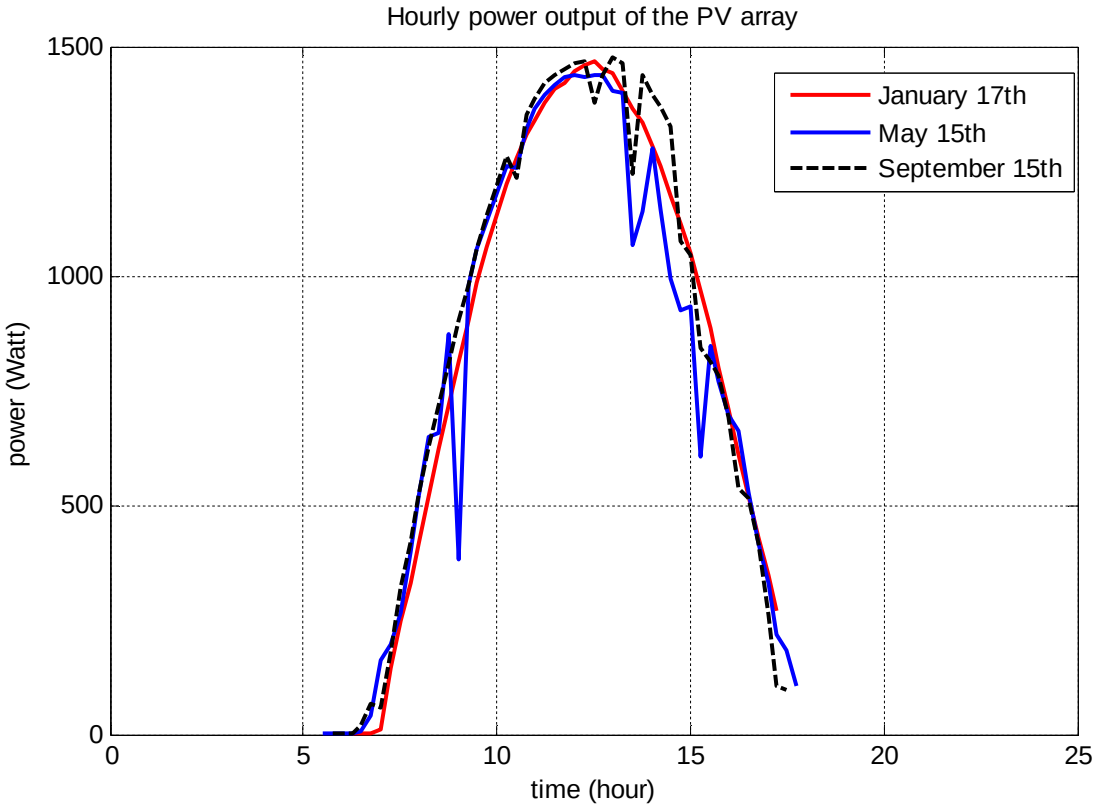

Figure 5. 17 - The PV array hourly power output

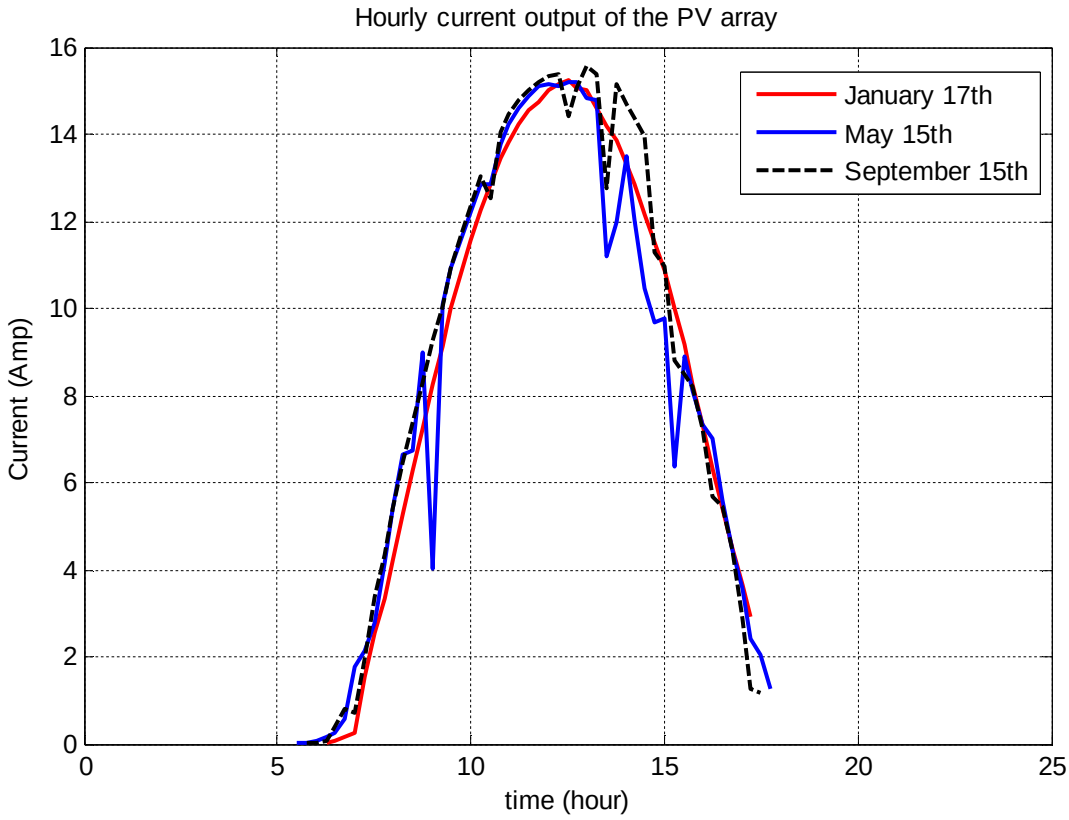

Figure 5. 18 - The PV Array Hourly Current Output

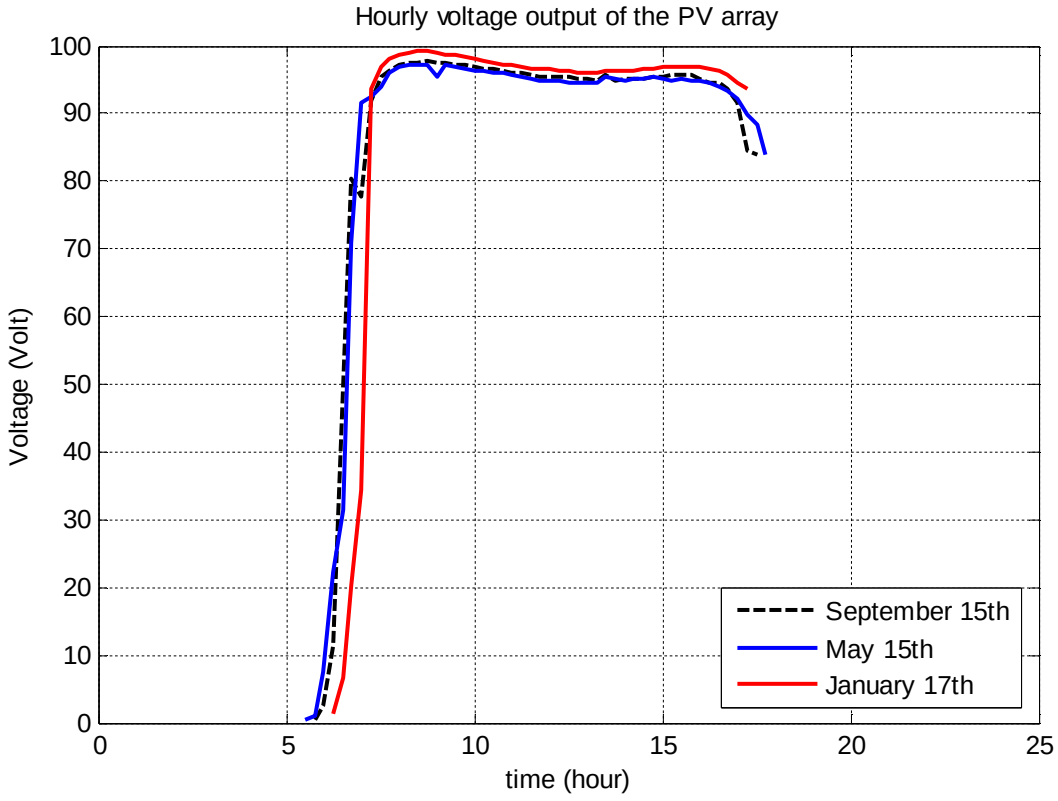

Figure 5. 19 - The PV Array Hourly Voltage Output

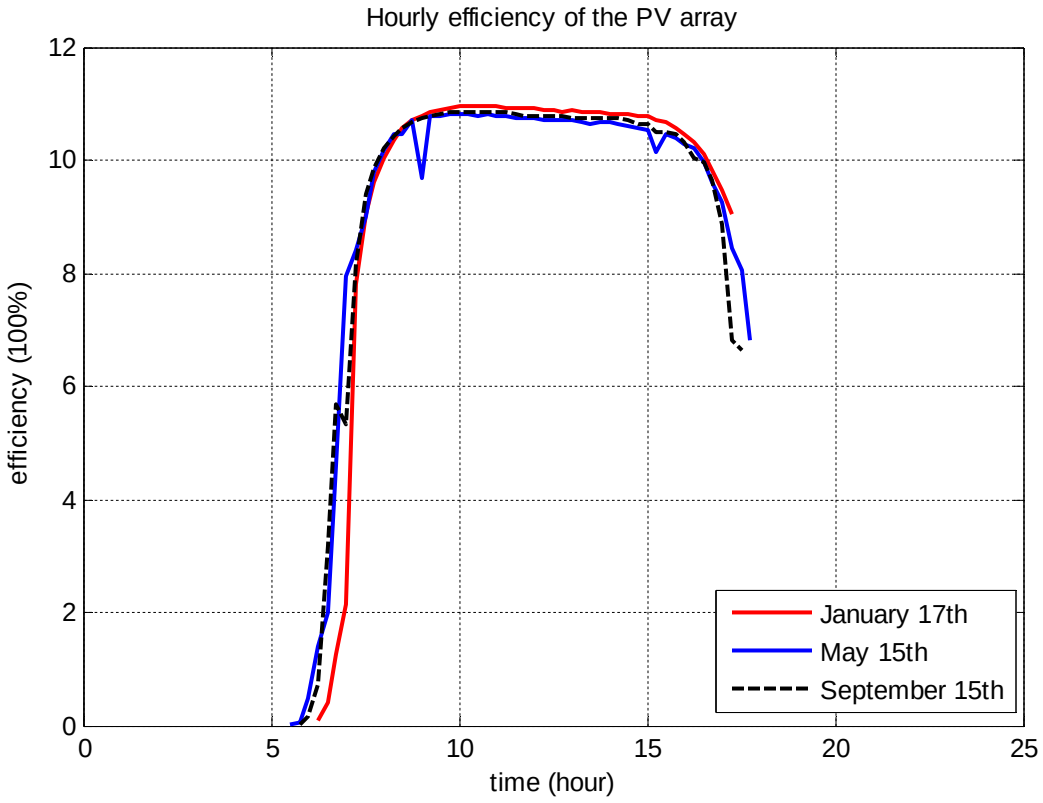

Figure 5. 20 - The PV Array Hourly Efficiency Variation

The above four Figures (Figure 5.17 – 5.20) shows the performance simulation of the selected *Siemens PowerMax* solar cells, *solar module SP75*, to show the hourly variation of power, voltage, current and efficiency of the PV panel using the real weather data in our case Jigjiga. The output power resulted from this simulation are the main input parameter to the pump equation, to evaluate the hourly performance simulation of our system. The pump characteristic equation result depends on the panel output result analyzed here. The overall efficiency of the system can also identified.

5.8. Hourly Performance Variation of the PVPWP System

In this section the overall system hourly performance will be simulated. The objective of this thesis is analysis and hourly performance simulation of solar powered water pumping system. This study takes place for Jigjiga real weather conditions to determine and model the operating points of the PVPWP system.

Maximum power point tracking MPPT control is integrated to the system to minimize the fluctuation of the suppled power to the pump motor, since adding MPPT control improve PV performance than the direct coupling system. The input power of the pump motor are 1400W which generate from PV panel. When the PV panel generates more power than the required one, the system continue running without any interruption and the pump deliver its maximum performance. The

selected motor supplied with a voltage of 30-300V, when the voltage reaches below or above the required voltage the controller will shut down the system and protect it from failure.

Daily flow rate output or the expected discharge of the system depends on the daily solar radiation. The modeled system shows the hourly variation of the flow rate in different pumping head (50, 60, 70, 80 and 90 meter). As the pumping head increases the flow rate decreases as shown in Figure 5.21, at MPPT of the system the pump flowrate remains constant. Constant working points of the pump shown in the Figure are the maximum flow rate hours to pump the water to the reservoir throughout a day. This modeling are checked for different days of a year, Figure 5.21 is for only the 17th day of January to minimize a repeated graphical representations, for the months of May and September the graphs are presented in (Appendix C).

The result of PVPWP system modeling presented hear shows the hourly flow rate capacity we can get from the system in different pumping system head in different seasons of the year. For instance at the month of January, for head H of 50 m - 90 m flow rate Q varies between 3.25 m^3/hr – 2.95 m^3/hr as indicated in the Figure, for the time period from 9AM to 4PM of the selected days. Thanks to the MPPT control system, the pump duty point is continuously optimized according to the input power available. MPPT is only for pumps connected to DC supply. The wide voltage range enables the motor to operate at any voltage from 30 to 300 VDC or 90 to 240 VAC.

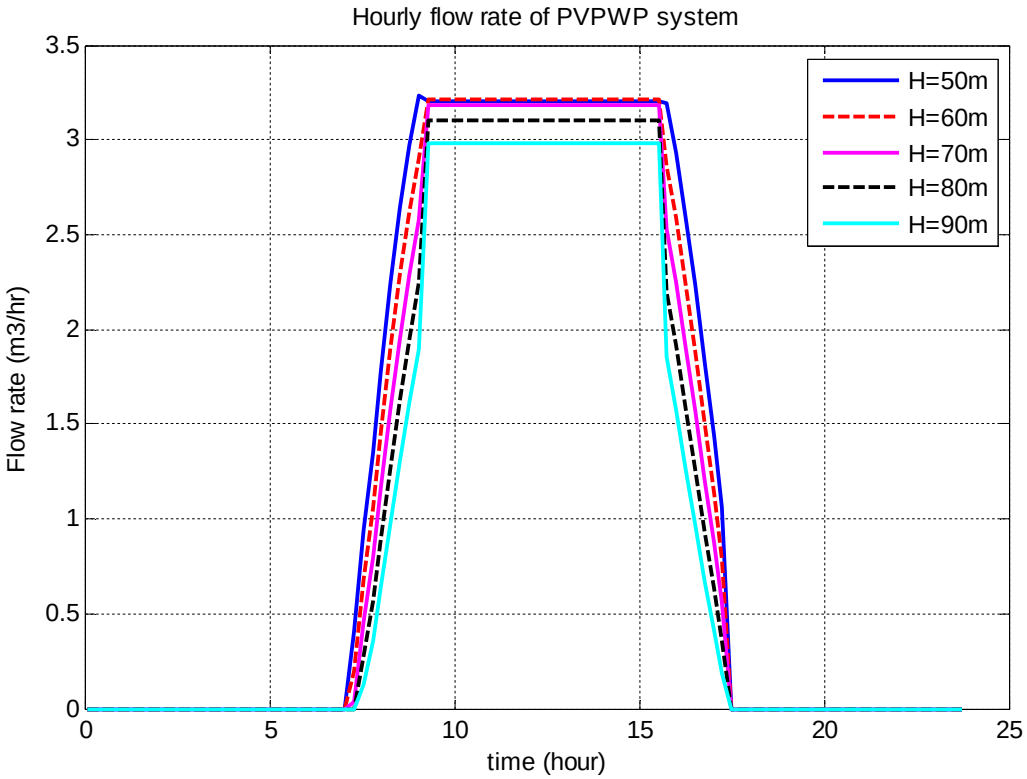

Figure 5. 21 - Hourly Flow Rate Output of the PVPWPS for January 17th in Different Head

Figure 5.22 shows head loss or frictional loss variation due to variation of the output flow rate. This head loss is the sum of a loss in a straight pipe, which deliver the water to the reservoir, and a loss in fittings we use in the system. For this modeling system we use 2 1/2" pipes and three elbows up to the inlet of the reservoir. As the Figure indicates the head loss increases as the flow rate increases and increase in total head of the system. Since the flow is laminar flow the friction loss calculated hear are very small and almost negligible.

Pump efficiency varies as shown in Figure 5.23, reaches its maximum when the pump flow rate reaches its constant point. At MPPT the efficiency becomes U shaped as shown in the Figure. For different working head and flow rate of the system the pump efficiency will vary and reaches its maximum points. Thus we can conclude that, the pump works in its best efficiency points as a working head increases, for instance at month of January at H = 60m the efficiency reaches 60% as flow rate Q = 3.1 m^3/hr for the time period from 9AM to 4PM of the selected days of the months.

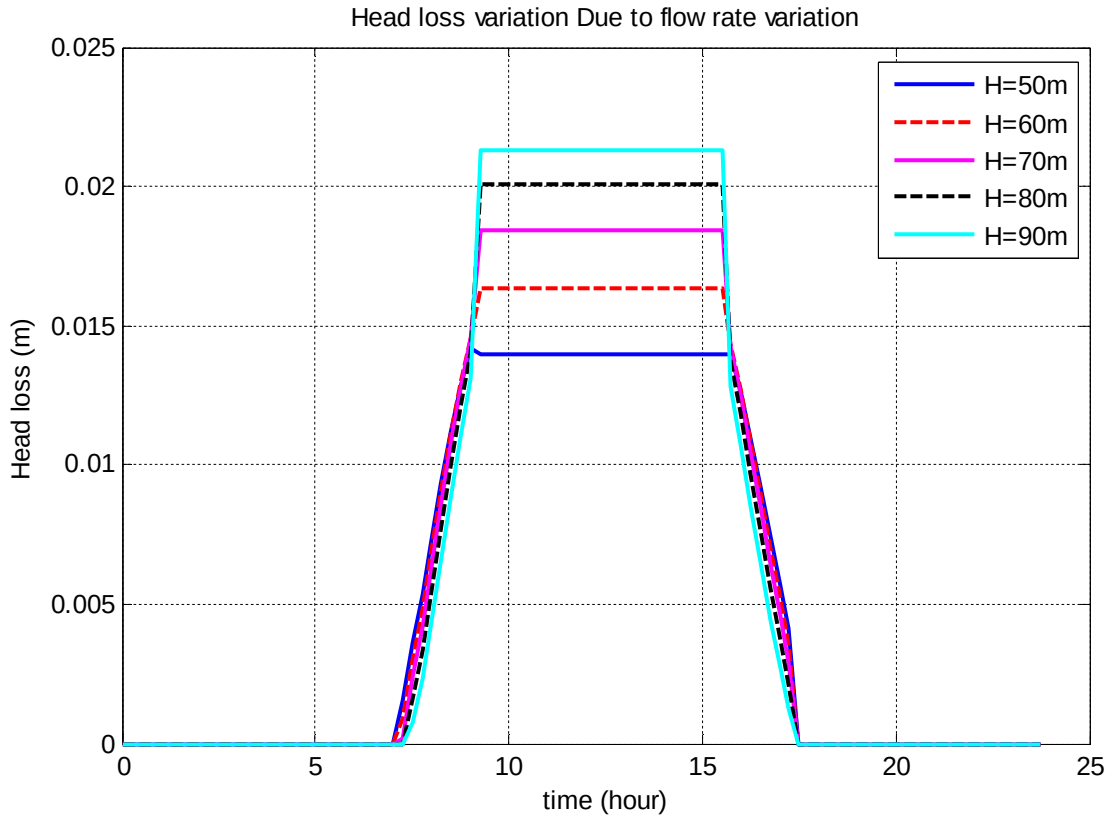

Figure 5. 22 - Pump Head Loss Due to Flow Rate Variation for January 15th in Different Total Head

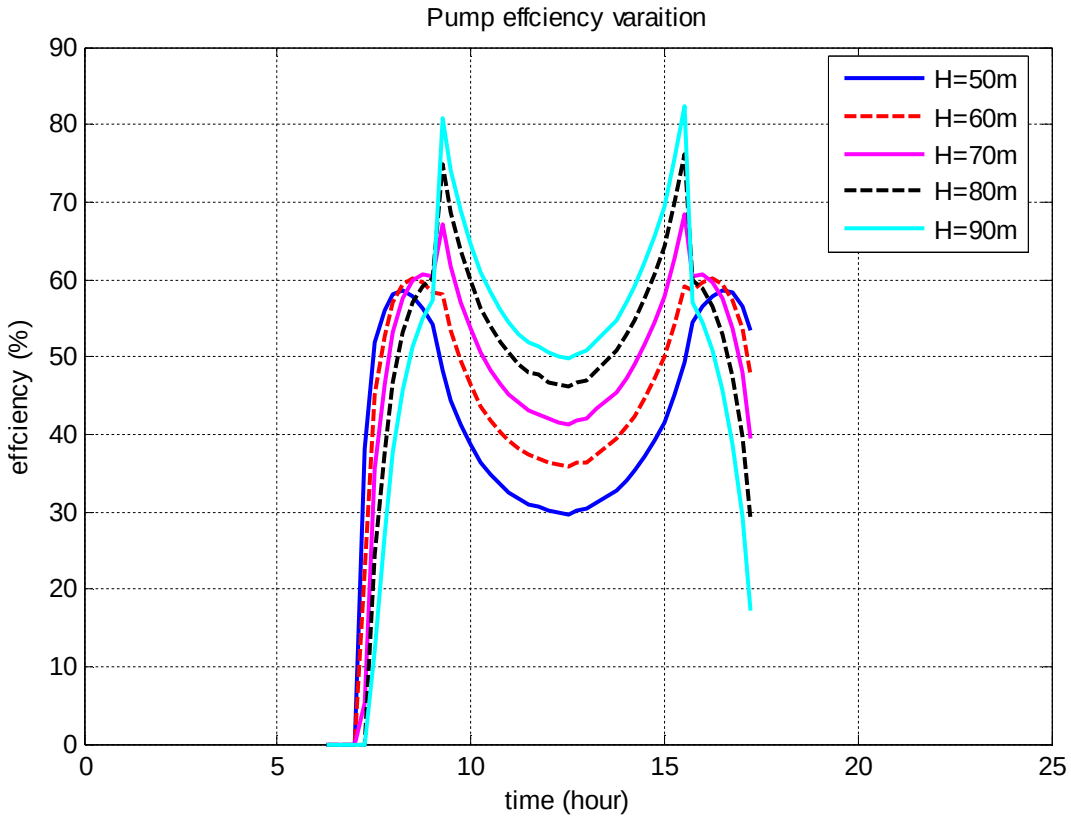

Figure 5. 23 - Pump Efficiency Variation for January 17th in Different Total Dynamic Head

The result of PVPWP system modeling presented hear shows the hourly flow rate capacity we can get from the system in different pumping system head in different seasons of the year. For instance at the month of January, for head H of 50 m - 90 m flow rate Q varies between 3.25 m^3/hr – 2.95 m^3/hr as indicated in the Figure, for the time period from 9AM to 4PM of the selected days and available solar irradiance.

Comparing the output flowrate result of this modeling with the experimental analysis made in Madinah site located in Saudi Arabia using curve fitting characteristic equation generated by the authors [18]. The experimental data are obtained and performances was calculated using the measured meteorological data of Madinah site located in Saudi Arabia. The PVWPS is composed by: photovoltaic generator of 1.8 KW, submersible helical pump of type SQF, flow meter of type Electromagnetic, built-in microprocessor with MPPT control and Agilent data logger system connected to computer for data acquisition. The PVWPS is installed in a well of 120m of depth. Powered by the selected PV array, the pump is tested for a fixed head of 80 m during sunny days.

As the graph below shows the comparison of the experimental analysis made and our simulation model result of the pumping system for 80m total head, flow rate (m^3/day) and irradiation (Wh/m^2/day). Within a range of 5000-7000 Wh/m^2/day solar irradiation the modeled simulation

result gives a flow rate of 20-30 m^3/day at a total head of 80m for sunny days. This simulation result was compared to the experimental analysis made as the curves shown in Figure 5.24 below. The dotted curve shows the curve fitting results of an experimental analysis and the bold line shows the model simulation result.

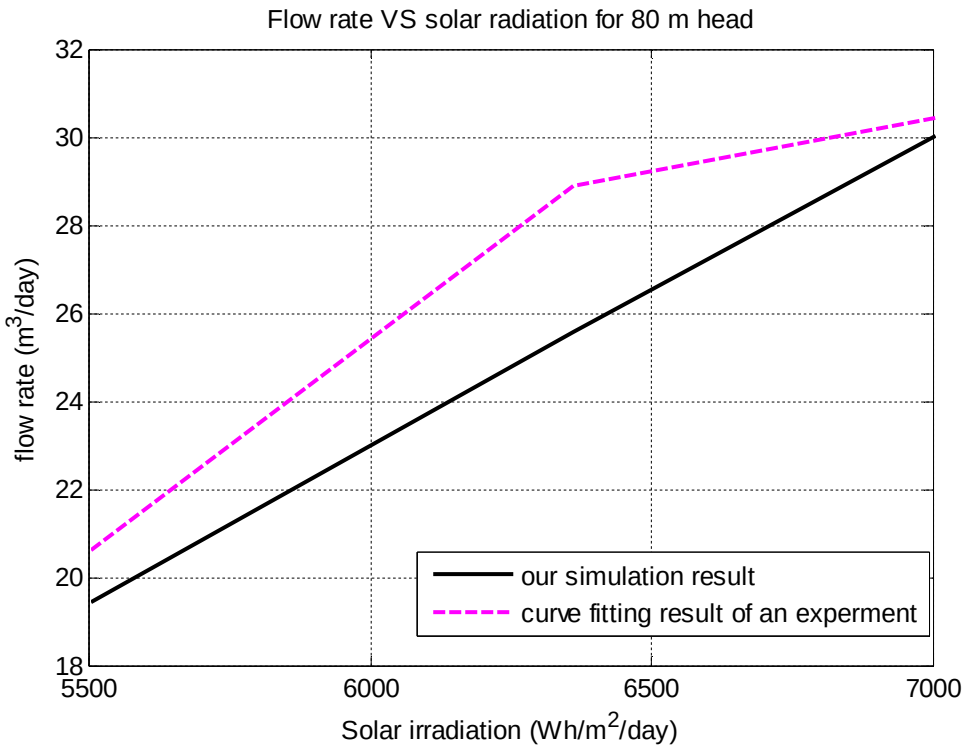

Figure 5. 24 – Pump Flowrate Comparison with Experimental Analysis

CHAPTER SIX

6. CONCLUSION AND RECOMMENDATION

6.1. Conclusion

The In this thesis a solar powered water pumping system, which is coupled to a PV panel is analyzed and simulated under real weather condition for different seasons. SQF helical type submersible pump which is a heart of the pumping system is selected and 24 units of SP75 solar module of 1800 watt (each module generates 75W) non-tracking PV array (with 6Sx4P configuration) are selected to generate the required power, voltage and current output to the pump motor. Maximum power point tracking (MPPT) controller which optimizes the power output of the PV module are integrated to improve system power.

The automatically measured data from National Metrology Agency for global radiation and temperature for Jigjiga, are analyzed using Matlab. Thus, evaluating and comparing the raw data measured using Pyranometer on horizontal plane with an optimally tilted panel. The data obtained from the agency are measured using Pyranometer in every 15 minutes (which is 96 data for each day) automatically for both solar radiation in (W/m^2) and temperature in (^oC). Change the measured radiation data which is measured on horizontal surface into expected radiation intensity on the optimally tilted panel, compare incident angle of our tilted panel to zenith angle and calculate cell temperature. This analysis result gives us the required data provide us electrical power output from the solar module (like voltage, current and power output).

The manufacture of the pump provide only the graphical data and technical specification of the pump and motor. Using this manufacturer curve, generate flowrate values in different power and head variation as shown in (Appendix A-1.2). By means of curve and surface fitting polynomial function, using this power, flowrate and head data, we generate characteristics equations which determines the performance of the pumping system at different operating conditions. By incorporating the long pump performance equation generated with a simple electrical correlation (which is $power = current \times Voltage$) the hourly flow characteristics of the pump was determined for each flow rate variations throughout a day.

The performance simulation of the selected solar cells, *solar module SP75*, detailed electrical characteristics of 1800 watt non-tracking PV array (with 6Sx4P configuration) determined on current vs. voltage as well as power vs. voltage plane by taking manufacturer's data sheet of the PV module as input, to show the hourly variation of power, voltage, current and efficiency of the PV

panel using the real weather data in Jigjiga. The efficiency of the PV panel reaches its maximum point during maximum solar radiation time and stay almost constantly during this maximum radiation time. The output power resulted from PV analysis was the main input parameter to the pump characteristic equation, to evaluate the hourly performance PVPWP system, thus the operating flow rate of the pump was determined. So that we can have all information about the performance of the solar water pumping system, for every 15 minutes at which environmental data such as global radiation and ambient temperature had been taken. In this fashion an hourly variation in performance of the solar water pumping system was modelled. It is observed that the pump starts to run at its minimum power input, when the radiation intensity on the tilted panel reaches around 20 W/m2 in the morning time, and the pump starts to run at its maximum capacity when solar radiation intensity on the tilted panel passes approximately 700W/m^2 as shown in Figures in chapter 6 for the time period from 10AM to 3PM of the selected days.

The result of PVPWP system modeling presented hear identifies the hourly flow rate capacity we can get from the system in different pumping system head in different seasons of the year. For instance at the month of January, for head H of 50 m - 90 m flow rate Q varies between 3.25 m^3/hr – 2.95 m^3/hr as indicated in the Figures. For different working head and flow rate of the system the pump efficiency will vary and reaches its maximum points. Also, the pump works in its best efficiency points as a working head increases, for instance at month of January at H = 60m the efficiency reaches 60% as flow rate Q = 3.1 m^3/hr for the time period from 9AM to 4PM of the selected days.

Hence, it is concluded that the performance of the system integrated with maximum power point tracking (MPPT) controller, which optimizes the power output of the PV module, gets higher for the time period of a day in which the radiation intensity gets higher which results a higher flowrate of the pumping system which intern results a higher system performance.

The validation was made with the experimental analysis made using curve fitting characteristic equation at total dynamic head of 80m and solar irradiation of 5000-7000 Wh/m^2/day. The modeled simulation result gives a flow rate of 20-30 m^3/day for sunny days. The flow rate capacity per day of the simulation result was compared to the experimental analysis made and there is a little difference since the experiment is done under weather condition of Madinah, Saudi Arabia.

6.2. Recommendation

The adoption of self-sustaining water pumping system practices using solar energy resources are an essential element for the development of communities. Modeling PVPWP system in its best performance in real weather condition gives a required output results. Actual system implementation shall be tested in the study area for selected sites. In addition modeling this system using wind energy is the other option to model the water pumping system in rural areas. In this thesis PVPWP system was evaluated with 6Sx4P PV array configuration. Evaluating this system with different PV array configuration my give different output results.

REFERENCE

[1] "Ethiopia Access to Electricity." [Online]. Available: https://tradingeconomics.com/ethiopia/access-to-electricity-percent-of-population-wb-data.html.

[2] T. E. Benefi and I. W. Management, "MAKING WATER A PART OF ECONOMIC DEVELOPMENT" The Economic Benefi ts of Improved Water, 2005.

[3] A. Curbelo, "UNESCO ' s Global Renewable Energy Education and Training Programme in Latin America View," *Sci. Forum*, pp. 25–37, 2004.

[4] O. Benchikh, "UNESCO s Global Renewable Energy Education and Training Programme (GREET Programme)," *Sci. Forum*, 2004.

[5] A. M. Z. & M. N. Eskander, "Matching of Photovoltaic Motor-Pump System for Maximum Efficiency Operation," pp. 279–288, 1996.

[6] A. Nasir, "Design , Simulation and Analysis of Photovoltaic Water Pumping System for Irrigation of a Potato Farm at Gerenbo," 2016.

[7] M. S. Kyi, L. Maw, and H. M. Tun, "Study Of Solar PV Sizing Of Water Pumping System For Irrigation Of Asparagus," vol. 5, no. 06, pp. 71–75, 2016.

[8] S. Biswas and M. T. Iqbal, "Dynamic Modelling of a Solar Water Pumping," vol. 2018, 2018.

[9] A. Allouhi, M. S. Buker, A. Boharb, M. B. Amine, T. Kousksou, and A. Jamil, "PV water pumping systems for domestic uses in remote areas: Sizing process, simulation and economic evaluation," *Renew. Energy*, 2018.

[10] M. Aliyu, G. Hassan, I. M. Elamin, S. A. Said, M. U. Siddiqui, and A. T. Alawami, "A review of solar-powered water pumping systems," *Renew. Sustain. Energy Rev.*, vol. 87, no. August 2017, pp. 61–76, 2018.

[11] S. S. Chandel, M. N. Naik, and R. Chandel, "Review of solar photovoltaic water pumping system technology for irrigation and community drinking water supplies," *Renew. Sustain. Energy Rev.*, vol. 49, pp. 1084–1099, 2015.

[12] S. S. Chandel, M. N. Naik, and R. Chandel, "Review of performance studies of direct coupled photovoltaic water pumping systems and case study," *Renew. Sustain. Energy Rev.*, vol. 76, no. February, pp. 163–175, 2017.

[13] M. Jagan, M. Rao, M. K. Sahu, and P. K. Subudhi, "PV BASED WATER PUMPING SYSTEM FOR," *Mater. Today Proc.*, vol. 5, no. 1, pp. 1008–1016, 2018.

[14] A. K. Tiwari and V. R. Kalamkar, "Effects of total head and solar radiation on the performance of solar water pumping system," *Renew. Energy*, vol. 118, pp. 919–927, 2018.

[15] M. Benghanem, K. O. Daffallah, and A. Almohammedi, "Results in Physics Estimation of daily flow rate of photovoltaic water pumping systems using solar radiation data," *Results*

Phys., vol. 8, pp. 949–954, 2018.

[16] B. S. Pali and S. Vadhera, "A novel solar photovoltaic system with pumped-water storage for continuous power at constant voltage," *Energy Convers. Manag.*, vol. 181, no. December 2018, pp. 133–142, 2019.

[17] E. E. Aboul, A. M. Zaki, and M. M. El-sotouhy, "Design and control of a standalone PV water pumping system," *J. Electr. Syst. Inf. Technol.*, vol. 4, no. 2, pp. 322–337, 2017.

[18] M. Benghanem, K. O. Daffallah, S. N. Alamri, and A. A. Joraid, "Effect of pumping head on solar water pumping system," *Energy Convers. Manag.*, vol. 77, pp. 334–339, 2014.

[19] M. Benghanem, K. O. Daffallah, A. A. Joraid, S. N. Alamri, and A. Jaber, "Performances of solar water pumping system using helical pump for a deep well : A case study for Madinah , Saudi Arabia," *Energy Convers. Manag.*, vol. 65, pp. 50–56, 2013.

[20] A. Allouhi *et al.*, "PV water pumping systems for domestic uses in remote areas : Sizing process , simulation and economic evaluation," *Renew. Energy*, vol. 132, pp. 798–812, 2019.

[21] R. Paper, "REVIEW PAPER SOLAR ENERGY INSTALLATIONS FOR PUMPING IRRIGATION WATER," vol. 21, pp. 255–262, 1978.

[22] Q. Kou, S. A. Klein, and W. A. Beckman, "A method for estimating the long-term performance of direct-coupled pv pumping systems," vol. 64, no. 98, pp. 33–40, 1998.

[23] K. Kapadia, "Productive uses of renewable energy A Review of Four Bank-GEF Projects Kamal Kapadia Consultant January 2004," no. January, 2004.

[24] R. E. Katan and C. V Nayar, "Performance Analysis of a Solar Water Pumping System," pp. 81–87, 1996.

[25] C. Protogeropoulos and S. Pearce, "LABORATORY EVALUATION AND SYSTEM SIZING CHARTS FOR A ' SECOND GENERATION ' DIRECT PV-POWERED , LOW COST SUBMERSIBLE SOLAR PUMP," vol. 68, no. 5, pp. 453–474, 2000.

[26] E. R. Group, "Solar energy vision for Ethiopia," 2012.

[27] Revolvy, "Renewable energy in Ethiopia." 2018.

[28] A. W. Worqlul *et al.*, "Assessing potential land suitable for surface irrigation using groundwater in Ethiopia," *Appl. Geogr.*, vol. 85, pp. 1–13, 2017.

[29] A. September, "Renewable Energy Water Pumping Systems Handbook," no. July, 2004.

[30] A. I. N. Press, "Approaches for developing a sizing method for stand-alone PV systems with variable demand," vol. 33, pp. 1037–1048, 2008.

[31] J. A. Duffie, *Solar Engineering of Thermal Processes*, Second Edi. John Wiley & Sons, 1980.

[32] M. Elrefai and R. A. Hamdy, "Design and Performance Evaluation of a Solar Water Pumping System : A Case Study," no. December, 2016.

[33] R. Foster and A. Ellis, “Renewable Energy for Water Pumping Applications in Rural Villages Period of Performance,” no. July, 2003.

[34] H. H. Bengtson, “Spreadsheet Use for Pipe Flow- Friction Factor Calculations,” 2003.

[35] I. J. Karassik, J. P. Messina, W. H. Fraser, and I. J. Karassik, *Pump Handbook*, Third Edit. McGRAW-HILL, 2001.

[36] M. G. Villalva, J. R. Gazoli, and E. R. Filho, “Comprehensive Approach to Modeling and Simulation of Photovoltaic Arrays,” vol. 24, no. 5, pp. 1198–1208, 2009.

[37] A. Gupta, A. Khare, and A. Shrivastava, “Modeling of Solar Photovoltaic Module and Effect of Variation of Insolation Using Matlab / Simulink,” 2014.

[38] & V. K. G. Vineet Singla, “MODELING OF SOLAR PHOTOVOLTAIC MODULE & EFFECT OF INSOLATION VARIATION USING MATLAB / SIMULINK,” pp. 5–9, 2013.

[39] D. Rusirawan and I. Farkas, “Identification of model parameters of the photovoltaic solar cells,” *Energy Procedia*, vol. 57, pp. 39–46, 2014.

[40] S. Bana and R. P. Saini, “Identification of unknown parameters of a single diode photovoltaic model using particle swarm optimization with binary constraints,” *Renew. Energy*, vol. 101, pp. 1299–1310, 2017.

[41] S. Ziyad, *Renewable Energy System Design*. Elsevier Inc, 2014.

[42] R. Araneo, U. Grasselli, and S. Celozzi, “Assessment of a practical model to estimate the cell temperature of a photovoltaic module,” 2014.

[43] A. Luque and S. Hegedus, *Hand book of Photovoltaic Science*. John Wiley & Sons Ltd, 2003.

[44] G. M. Masters, "*Renewable and Efficient Electric Power Systems"*, John Wiley & Sons, 2004.

[45] S. A. Kalogirou, "*Solar Energy Engineering Processes and Systems"*, Second Edi. Elsevier, INC, 2014.

[46] “Chapter E02 Curve and Surface Fitting,” in *Product data sheet*, pp. 1–20.

[47] S. C. Chapra and R. P. Canale, *Numerical Methods for Engineers*, Seventh Ed. McGraw-Hill Science/Engineering/Math, 2013.

[48] C. W. C. & J. G. HAYES, “Curve and Surface Fitting,” no. x, pp. 164–183, 1965.

[49] www.mathworks.com, “Curve and Surface Fitting - MATLAB & Simulink.” .

[50] S. A. Klein, “REVIEW PAPER CALCULATION OF MONTHLY AVERAGE INSOLATION ON TILTED SURFACES,” vol. 19, pp. 325–329, 1977.

[51] G. D. Booklet, “SQFlex DATA BOOKLET,” 2019.

[52] S. S. GmbH, “Solar Module SP75.”

[53] Tamer Khatib and W. Elmenreich, "*MODELING OF PHOTOVOLTAIC SYSTEMS USING MATLAB"*, WILEY, 2016.

APPENDIX

Appendix A – Pump Specification

Appendix A-1.1 - SQF 2.5-2 N 50 Hz manufacturer performance curve

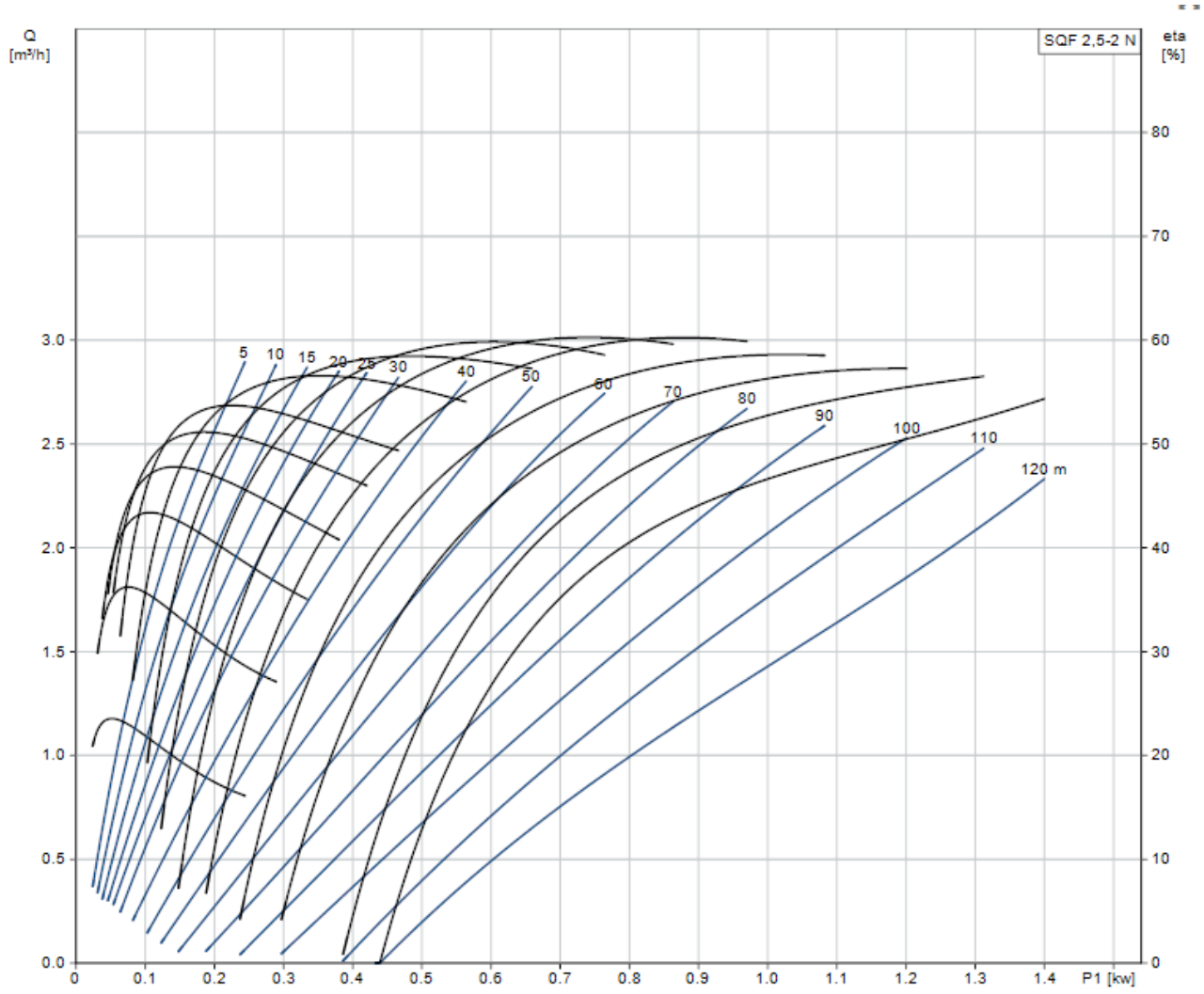

Appendix A-1.2 - SQF 2.5-2 N Pump Flow Rate at Different Head and Power input

P (kw)	Q_1(m3/hr)	Q_2 (m3/hr)	Q_3 (m3/hr)	Q_4 (m3/hr)	Q_5 (m3/hr)
	50m	60m	70m	80m	90m
0.1	0.16	-	-	-	-
0.12	0.24	0.10	-	-	-
0.15	0.41	0.22	0.07	-	-
0.2	0.70	0.47	0.26	0.11	-
0.25	0.95	0.69	0.46	0.32	0.11

0.3	1.22	0.94	0.66	0.44	0.28
0.35	1.48	1.17	0.84	0.65	0.41
0.4	1.70	1.38	1.10	0.82	0.58
0.45	1.94	1.62	1.29	1.02	0.76
0.5	2.16	1.80	1.47	1.20	0.92
0.55	2.34	2.00	1.67	1.37	1.06
0.6	2.54	2.20	1.84	1.55	1.23
0.65	2.74	2.38	2.05	1.72	1.40
0.7	-	2.56	2.23	1.89	1.55
0.75	-	2.71	2.39	2.05	1.69
0.8	-	-	2.54	2.20	1.86
0.85	-	-	2.67	2.34	2.02
0.9	-	-	-	2.49	2.14
0.95	-	-	-	2.63	2.25
1	-	-	-	-	2.41
1.05	-	-	-	-	2.51

Appendix A-1.3 - SQF 2.5-2 N Manufacturer Specification

Description	Value
General information:	
Product name:	SQF 2,5-2 N
Product No:	95027331
EAN number:	5700834791765
Technical:	
Stages:	2
Approvals on motor nameplate:	CE,RCM,EAC
Pump No:	95027415
Valve:	pump with built-in non-return valve
Materials:	
Pump:	Stainless steel
	DIN W.-Nr. 1.4401
	AISI 316
Impeller:	DIN W.-Nr. 1.4401
Rotor:	Stainless steel
	DIN W.-Nr. 1.4401
	AISI 316
Stator:	Stainless steel / EPDM
	DIN W.-Nr. 1.4401
	AISI 316
Installation:	
Maximum ambient pressure:	15 bar
Pump outlet:	Rp 1 1/4
Minimum borehole diameter:	76 mm
Liquid:	
Pumped liquid:	Water
Maximum liquid temperature:	40 °C
Liquid temperature during operation:	20 °C
Density:	998.2 kg/m³
Electrical data:	

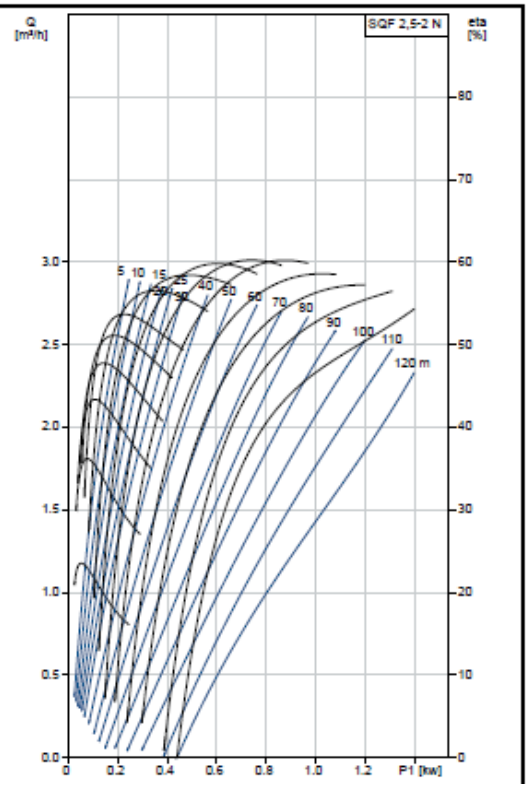

Electrical data:	
Motor type:	MSF3N
Power input - P1:	1.4 kW
Rated voltage ac:	1 x 90-240 V
Rated voltage dc:	30-300 V
Rated current:	8.4 A
Power factor:	1,0
Rated speed:	500-3600 rpm
Start. method:	direct-on-line
Enclosure class (IEC 34-5):	IP68
Insulation class (IEC 85):	F
Motor protec:	Y
Thermal protec:	internal
Length of cable:	2 m
Motor No:	96275337
Udc:	300 V
	30 V
Others:	
Minimum efficiency index, MEI ≥:	-.--
Net weight:	8.2 kg
Gross weight:	10 kg
Shipping volume:	0.024 m³
Sales region:	Europe/South America/Japan

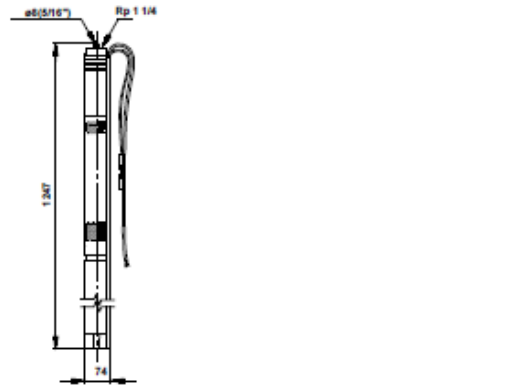

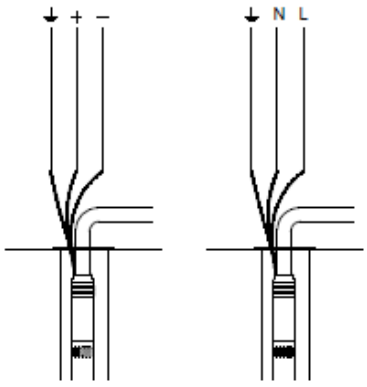

Printed from Grundfos Product Centre [2018.02.043]

Appendix B – Solar Module Specification

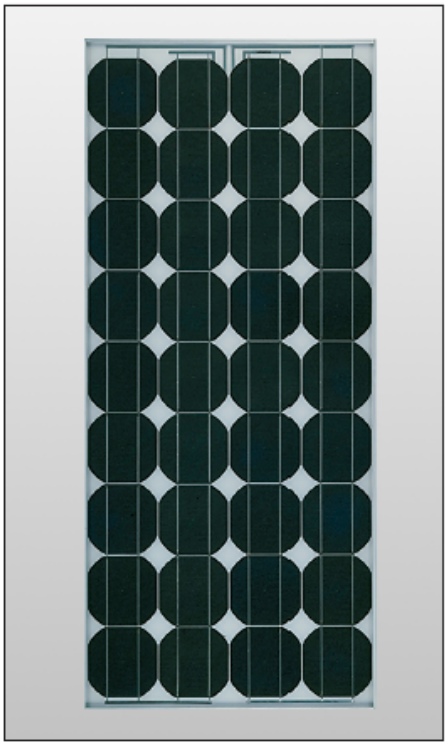

Solar module

Model:	**SP75**
Rated power:	**75 Watts**
Limited Warranty:	**25 Years**

Certifications and Qualifications

- UL-Listing 1703
- TÜV safety class II
- JPL Specification No. 5101-161
- IEC 61215
- CE mark
- FM Certification

Solar module SP75			
Electrical parameters			12 V/6 V
Maximum power rating P_{max}		[W_p] [1]	75
Rated current I_{MPP}		[A]	4.4/8.8
Rated voltage V_{MPP}		[V]	17.0/8.5
Short circuit current I_{SC}		[A]	4.8/9.6
Open circuit voltage V_{OC}		[V]	21.7/10.9
Thermal parameters			
NOCT [2]		[°C]	45 ±2
Temp. coefficient: short-circuit current			2.06 mA / °C
Temp. coefficient: open-circuit voltage			-.077 V / °C
Qualification test parameters [4]			
Temperature cycling range		[°C]	-40 to +85
Humidity freeze, Damp heat		[%RH]	85
Maximum system voltage		[V]	600 V per UL (1000 V per ISPRA)
Wind Loading	PSF	[N/m^2]	50 [2400]
Maximum distortion [3]		[°]	1.2
Hailstone impact	Inches	[mm]	1.0 [25]
	MPH	[m/s]	52 [v=23]
Weight	Pounds	[kg]	16.7 [7.6]

1) Wp (Watt peak) = Peak power
(Minimum Wp = 70 Watts)

Air Mass	AM = 1.5
Irradiance	E = 1000 W/m²
Cell temperature	T_C = 25 °C

2) Normal Operating Cell Temperature at:

Irradiance	E = 800 W/m²
Ambient temperature	T_U = 20 °C
Wind Speed	v_W = 1 m/s

3) Diagonal lifting of module plane
4) Per IEC 61215 test requirements
5) 12 volt configuration

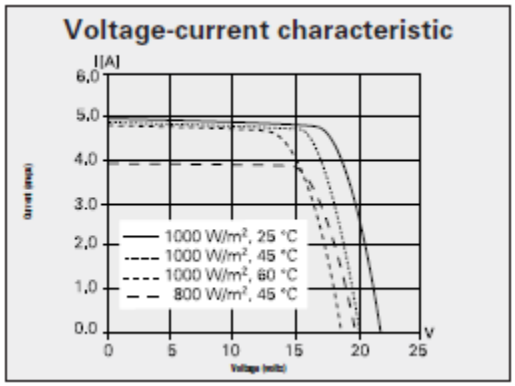

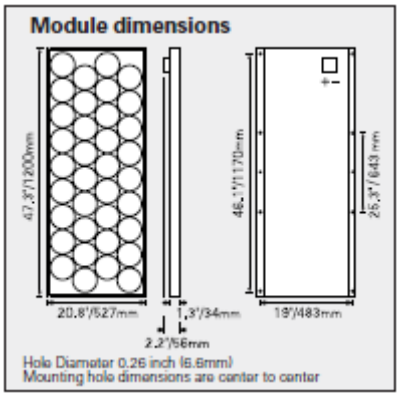

Appendix C – Hourly Performance Variation of the PVPWP System Curves

Hourly Flow Rate Output of the PVPWPS for May in Different Head

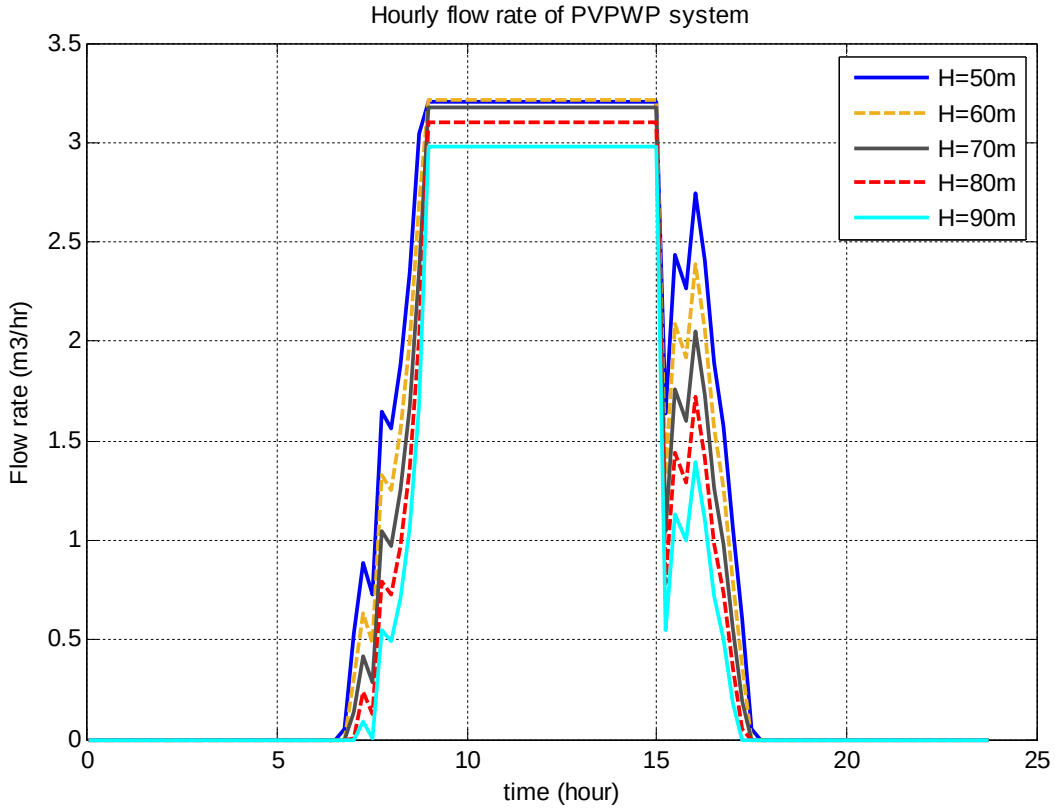

Pump efficiency variation for May in different head

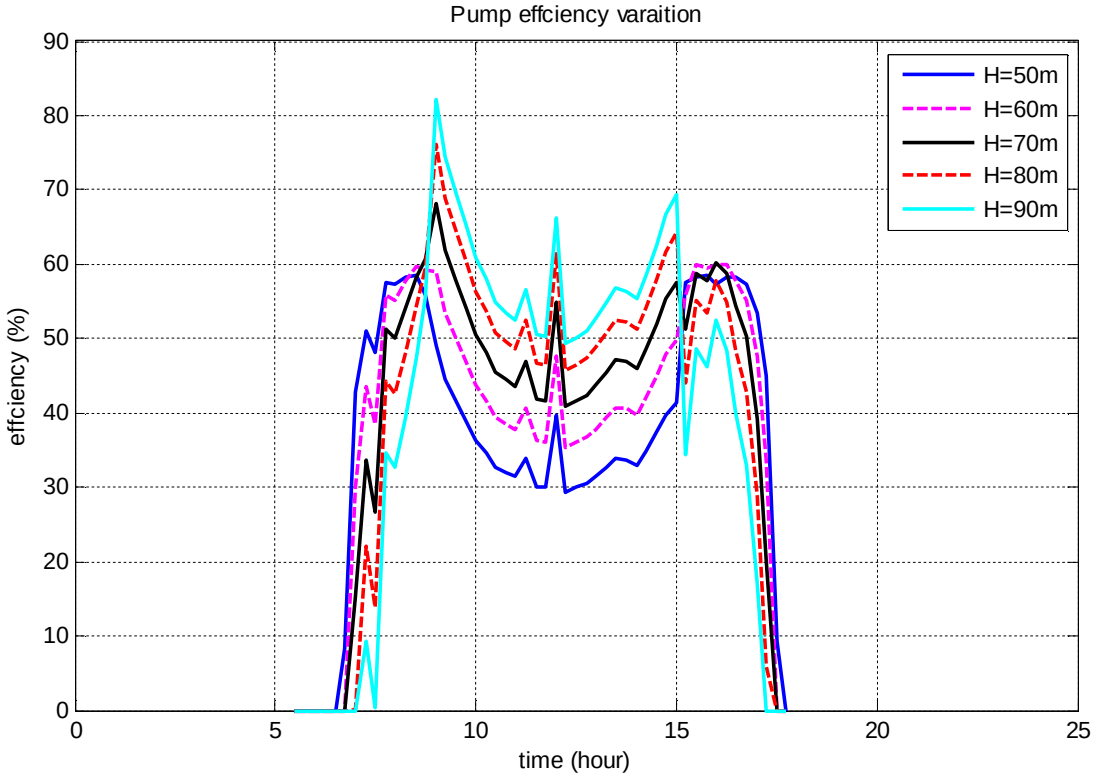

Hourly Flow Rate Output of the PVPWPS for September in Different Head

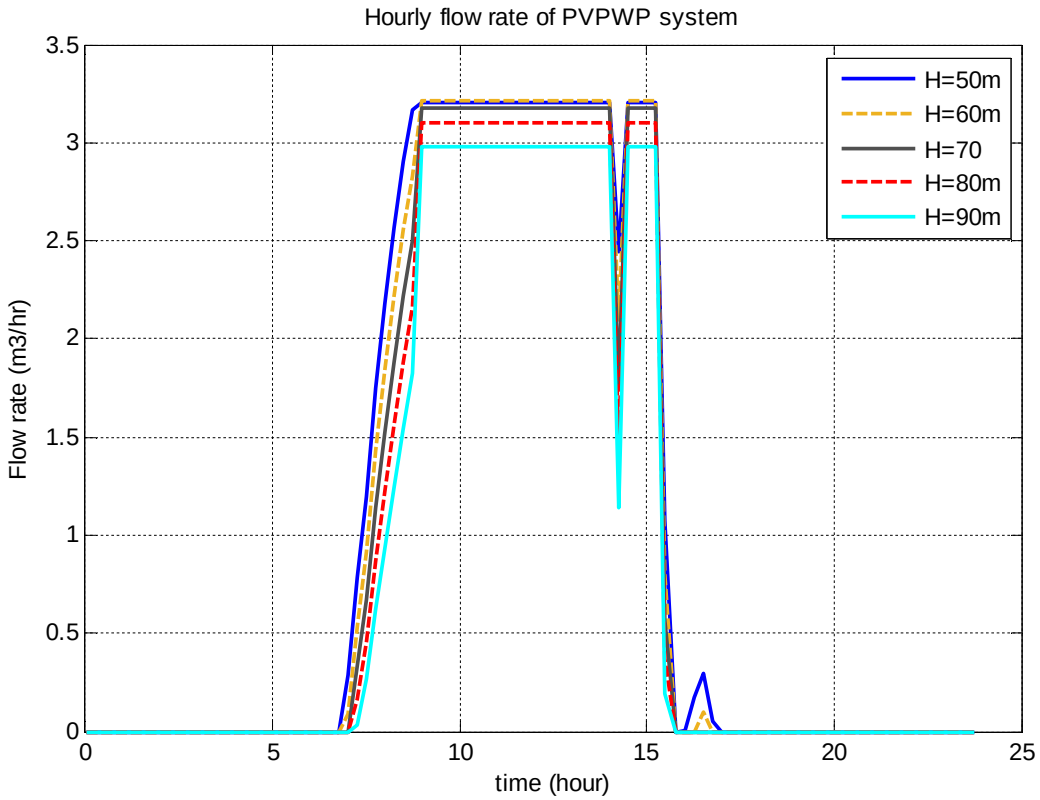

Pump efficiency variation for September in different head